

# Metal-Assisted Formation of Phosphorus–Oxygen Heterocyclic Complexes

Xiaoyong Sun,<sup>†</sup> Edward H. Wong,<sup>\*,†</sup> Mark M. Turnbull,<sup>\*,‡</sup> Arnold L. Rheingold,<sup>\*,§</sup> Beth E. Waltermire,<sup>§</sup> and Robert L. Ostrander<sup>§</sup>

Department of Chemistry, University of New Hampshire, Durham, New Hampshire 03824,  
Department of Chemistry, Clark University, Worcester, Massachusetts 01610, and  
Department of Chemistry, University of Delaware, Newark, Delaware 19716

Received June 9, 1994<sup>⊗</sup>

Starting with bis(dialkylamino)phosphine oxides or triphosphoxane  $[\text{R}_2\text{NPO}]_3$  rings, transition metal complexes containing  $\text{P}_4\text{O}_4$ ,  $\text{P}_5\text{O}_5$ , and  $\text{P}_6\text{O}_6$  heterocycles have been assembled. Specific products isolated were found to depend critically on reaction conditions, the metal, and its ancillary ligands, as well as the phosphorus substituent. While only monometallic products were obtained from divalent precursors of the nickel triad, bimetallic complexes were also produced from the group 6 metal carbonyls. In general, larger rings were obtained at higher temperatures. Only  $\text{P}_3\text{O}_3$  and  $\text{P}_4\text{O}_4$  products were formed around molybdenum, while  $\text{P}_5\text{O}_5$  structures could also be assembled about chromium, nickel, palladium, and platinum centers. One of the iron carbonyl complexes was found to feature an unusual  $\eta^1\text{-P}[\text{OP}(\text{O})]_2\text{P}$  ring, the product of a double POP to PP(=O) rearrangement. In addition, a dichromium  $\text{P}_6\text{O}_6$  cluster complex featuring the novel hexaphosphoxane ring was synthesized from bis(*cis*-2,6-dimethylpiperidino)phosphine oxide. Use of isolated monometallic  $\text{P}_n\text{O}_n$  complexes as ligands yielded heterobimetallic products as well as phosphoxane ring transfer reactions. The X-ray crystal structures of five representative complexes containing  $\text{FeP}_4\text{O}_4$  (**14**),  $\text{Cr}_2\text{P}_4\text{O}_4$  (**19a**, **19b**),  $\text{Cr}_2\text{P}_6\text{O}_6$  (**21**), and  $\text{MoFeP}_4\text{O}_4$  (**25**) cores, respectively, are reported.

## Introduction

Inorganic rings, cages, and clusters have relevance in many areas of chemical research including coordination, catalytic, polymer, and materials chemistry.<sup>1</sup> Trivalent phosphorus–oxygen heterocycles or cyclic phosphoxanes are potentially useful multidentate ligands that can lead to polycyclic, cage, or cluster complexes with  $\text{M}_m\text{P}_n\text{O}_n$  cores (Figure 1). We have previously shown that bis(dialkylamino)phosphine oxides and related triphosphoxane ( $[\text{R}_2\text{NPO}]_3$ ) rings are suitable precursors to  $\text{MP}_n\text{O}_n$  and  $\text{MP}_n\text{O}_n\text{M}$  complexes ( $\text{M} = \text{Cr}$ ,  $n = 4, 5$ ;  $\text{M} = \text{Mo}$ ,  $n = 3, 4$ ;  $\text{M} = \text{W}$ ,  $\text{Ni}$ ,  $\text{Pd}$ ,  $n = 4$ ) with bicyclic and cage structures (Figure 2A–F).<sup>2</sup> These syntheses depend critically on the presence of metal centers to provide templating sites for the linking up of  $\text{R}_2\text{NP}=\text{O}$  phosphinidene units. In this article, we will further expand the scope of these reactions and demonstrate the variety of products and structural types now accessible, including a novel hexaphosphoxane  $\text{Cr}_2\text{P}_6\text{O}_6$  cluster. Interesting ring transfer and metallaligand chemistry of several of these products will also be presented.

## Results

**Syntheses from Triphosphoxane ( $[\text{R}_2\text{NPO}]_3$ ) Rings. (1) The Nickel Triad.** In hexane, tris(diisopropylaminophosphoxane) ( $[\text{Pr}_2\text{NPO}]_3$ ) and various metal dihalide  $\text{MX}_2$  complexes ( $\text{MX}_2 = \text{NiCl}_2\cdot\text{DME}$ ,  $\text{NiBr}_2\cdot\text{DME}$ ,  $\text{PdCl}_2\cdot 2\text{PhCN}$ ,  $\text{PdBr}_2\cdot 2\text{PhCN}$ ,  $\text{PtCl}_2\cdot\text{NBD}$ ) all yielded tetraphosphoxane  $\text{MX}_2[\text{Pr}_2\text{NPO}]_4$  complexes (**1A,B**, **2A,B**, **3**). These light-yellow to orange-red solids have been characterized by IR, <sup>31</sup>P (Table 1), and, in some cases, <sup>1</sup>H and <sup>13</sup>C (Tables 2 and 3) NMR spectroscopy. The  $\text{NiBr}_2$  (**1B**),  $\text{PdCl}_2$  (**2A**), and  $\text{PdBr}_2$  (**2B**) products were also sufficiently stable for satisfactory elemental analyses to be obtained. The X-ray crystal structure of complex **2A** has been reported.<sup>2</sup> By <sup>31</sup>P NMR spectroscopy, the other palladium (**2B**) and platinum (**3**) products can also be assigned the same structure with a 1,5-chelating  $\text{P}_4\text{O}_4$  ring in a chair–chair conformation (Figure 2A), accounting for their  $\text{A}_2\text{X}_2$  spectra. The unique 1,3-ring coordination mode (Figure 2B) of the two nickel complexes (**1A,B**) can be deduced from their distinctive AA'XX' <sup>31</sup>P NMR (Table 1) spectra.<sup>2</sup>

Reactions using the tris(dicyclohexylaminophosphoxane) ( $[\text{Cy}_2\text{NPO}]_3$ ) precursor gave analogous  $\text{MX}_2\text{P}_4\text{O}_4$  products ( $\text{MX}_2 = \text{NiCl}_2$ , **4A**;  $\text{NiBr}_2$ , **4B**;  $\text{NiI}_2$ , **4C**;  $\text{PdCl}_2$ , **5A**;  $\text{PdBr}_2$ , **5B**;  $\text{PtCl}_2$ , **6**, but in addition,  $\text{MX}_2\text{P}_5\text{O}_5$  ( $\text{MX}_2 = \text{NiCl}_2$ , **7**;  $\text{PdCl}_2$ , **8A**;  $\text{PdBr}_2$ , **8B**; and  $\text{PtCl}_2$ , **9**) were also isolable under different reaction conditions. Specifically, reaction in hot toluene (90 °C) afforded unstable  $\text{NiCl}_2[\text{Cy}_2\text{NPO}]_4$  (**4A**; <sup>31</sup>P NMR, AA'XX' pattern) while room-temperature reaction in hexane yielded  $\text{NiCl}_2[\text{Cy}_2\text{NPO}]_5$  (**7**). A mixture of both (**4A**, **7**) was obtained by reaction at room temperature in toluene. In contrast, the palladium and platinum  $\text{P}_5\text{O}_5$  complexes (**8A,B**, **9**) were obtained from reactions in refluxing hexane while

<sup>†</sup> University of New Hampshire.

<sup>‡</sup> Clark University.

<sup>§</sup> University of Delaware.

<sup>⊗</sup> Abstract published in *Advance ACS Abstracts*, November 1, 1994.

(1) Armitage, D. A. *Inorganic Rings and Cages*; E. Arnold: London, 1972. Heal, H. G. *The Inorganic Heterocyclic Chemistry of Sulfur, Nitrogen, and Phosphorus*; Academic Press: London, 1980. Haiduc, I., Sowerby, D. B., Eds. *The Chemistry of Inorganic Homo- and Heterocycles*; Academic Press: London, 1987. Wollins, J. D. *Non-Metal Rings, Cages, and Clusters*; Wiley and Sons: New York, 1988. Mark, J. E.; Allcock, H. R.; West, R. *Inorganic Polymers*; Prentice Hall: New York, 1992.

(2) Wong, E. H.; Sun, X.; Gabe, E. J.; Lee, F. L.; Charland, J.-P. *Organometallics* **1991**, *10*, 3010.

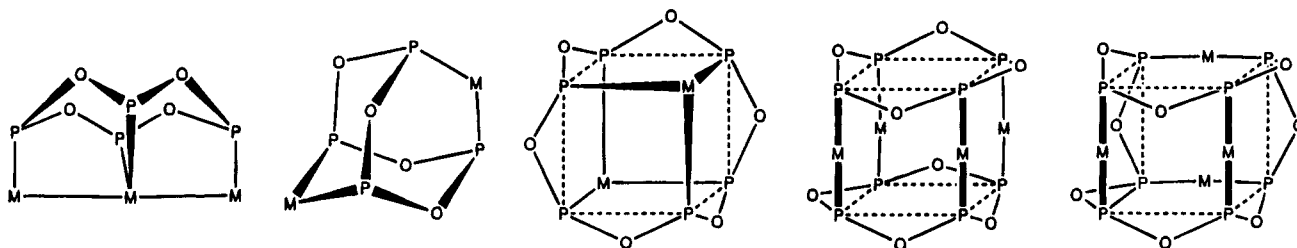


**Figure 1.** Possible structures based on  $M_m P_n O_n$  cyclic polyphosphoxane metal complexes ( $P = RP$ ).

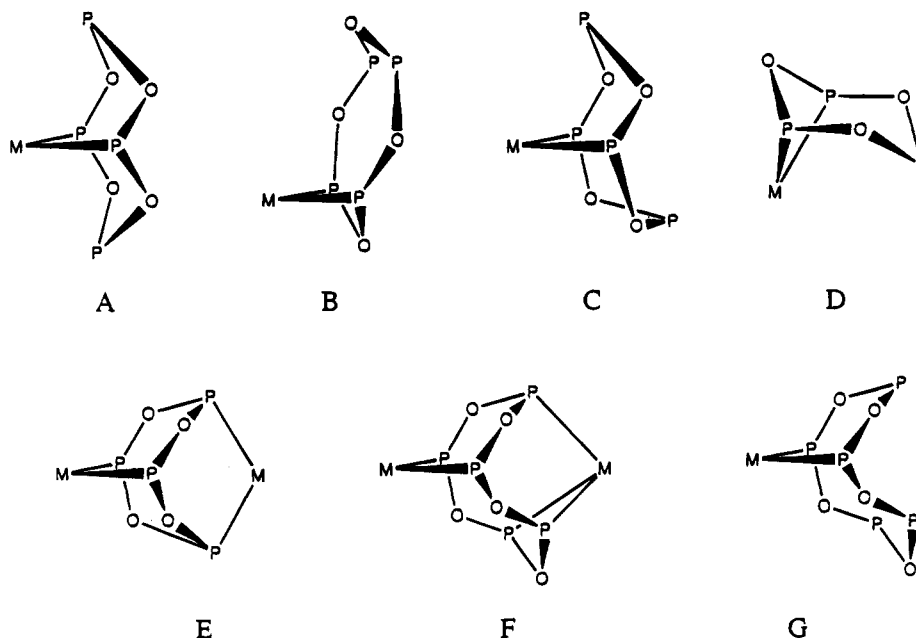


**Figure 2.** Bicyclic and cage structures of  $M P_n O_n$  and  $M_2 P_n O_n$  complexes ( $P = R_2 NP$ ).

the  $MP_4O_4$  products (**5A,B**, **6**) only formed in cold hexane at 4 °C.  $^{31}P$  NMR spectroscopy ( $A_2X_2$  patterns) supported similar structural assignments for the various  $MX_2P_4O_4$  complexes as made above for their diisopropylamino analogues. It also revealed the presence of two isomers of the  $PtCl_2[Cy_2NPO]_4$  complex, one with the familiar  $A_2X_2$  pattern (**6A**) and the second with an  $AMX_2$  pattern (**6B**). These can be assigned to the 1,5-chelated  $P_4O_4$  ring in chair–chair (Figure 2A) and boat–chair (Figure 2C) conformations, respectively. All the  $MX_2P_5O_5$  complexes exhibited  $AA'MXX'$  patterns consistent only with the novel 1,5-chelating  $\eta^2-P_5O_5$  coordination mode (Figure 2G).

**(2) Metal Carbonyls.** Room-temperature reaction of  $Mo(CO)_4(NBD)$  with  $[^iPr_2NPO]_3$  or  $[Cy_2NPO]_3$  in hexanes afforded the simple substitution products *cis*- $Mo(CO)_4[R_2NPO]_3$  ( $R = ^iPr, Cy$ ; **10A,B**, Figure 2D). These unstable white compounds slowly transformed to the known  $Mo(CO)_4[R_2NPO]_4Mo(CO)_4$  cage complexes (Figure 2E) in solution or in the solid state.<sup>2</sup> Similar reaction using  $Cr(CO)_4(NBD)$  required prolonged reaction times or refluxing to give *cis*- $Cr(CO)_4[R_2NPO]_4$  (**11a**) instead as a white solid. Its  $^{31}P$  NMR spectrum with an  $A_2XY$  pattern is consistent with a boat–chair 1,5-chelating mode for the tetraphosphoxane heterocycle (Figure 2C).

In refluxing toluene, diiron nonacarbonyl gave different products with the two triphosphoxanes. Specifically,  $[Cy_2NPO]_3$  yielded complex **12**,  $Fe(CO)_3[Cy_2NPO]_4$ , also with an  $A_2XY$   $^{31}P$  NMR spectrum (Table 1) as observed for the chromium complex **11** (Figure 2C). By contrast,

$[^iPr_2NPO]_3$  gave two isolable products in a 60:40 ratio; the first analyzed as  $Fe(CO)_3[^iPr_2NPO]_4$  (**13**) and the second as  $Fe(CO)_4[^iPr_2NPO]_4$  (**14**). Complex **13** can be assigned the chair–chair ligand ring conformation based on its  $A_2X_2$   $^{31}P$  NMR spectrum (Table 1, Figure 2A). Complex **14**, however, has a spectrum that indicated presence of high-field ( $\delta +24.5$ ) phosphoryl resonances in a distinctive  $AX_2Y$  pattern (Table 1). Its novel structure as revealed by an X-ray study (Figure 3) actually features a  $P[OP(=O)]_2P$  heterocycle as a monodentate ligand toward the tetracarbonyl iron.

**Syntheses from Bis(dialkylamino)phosphine Oxide Precursors.** We have previously reported the formation of complexes with  $MoP_3O_3$ ,  $MoP_4O_4$ ,  $Mo_2P_4O_4$ ,  $CrP_4O_4$ ,  $Cr_2P_4O_4$ ,  $Cr_2P_5O_5$ , and  $WP_4O_4$  (Figure 2A–F) cores from reactions of the respective metal hexacarbonyl and  $(^iPr_2N)_2P(O)H$ .<sup>2</sup> Similarly,  $(Cy_2N)_2P(O)H$  and  $Cr(CO)_6$  also produced two isomers of  $Cr(CO)_4[Cy_2NPO]_4$  with chair–chair (**11b**) and boat–chair (**11a**)  $P_4O_4$  conformations,  $Cr_2(CO)_8[Cy_2NPO]_4$  (**15**), and  $Cr_2(CO)_7-[Cy_2NPO]_5$  (**16**), with higher reaction temperatures favoring formation of the pentaphosphoxane complex **16** (Figure 2F). Traces of an unstable white solid characterized as the O-bonded  $Cr(CO)_5O=P(Cy_2N)_2H$  were also isolated ( $^{31}P$  NMR: singlet at  $\delta$  94.1,  $^1J_{PH} = 366$  Hz). Tungsten hexacarbonyl yielded  $W_2(CO)_7[Cy_2NPO]_5$  (**17**), a product analogous to **16**, although it was found to be quite unstable. In addition, prolonged reaction times led to isolation of small amounts of a red solid characterized as  $W_2(CO)_6[Cy_2NPO]_4$  (**18**), the  $^{31}P$  NMR spectrum of which contained a very low-field

Table 1.  $^{31}\text{P}\{^1\text{H}\}$  NMR Spectra of the Cyclic Phosphoxane Complexes<sup>a</sup>

complex		splitting pattern [chemical shift, ppm] ( <i>J</i> , Hz)
NiCl <sub>2</sub> [Pr <sub>2</sub> NPO] <sub>4</sub> ( <b>1A</b> )	AA'XX'	[ $\delta_A = \delta_{A'} = 144.2, \delta_X = \delta_{X'} = 55.7$ ] ( $J_{AA'} = J_{XX'} = 50, J_{AX} = J_{A'X'} = 20, J_{AX'} = J_{AX} = 1$ )
NiBr <sub>2</sub> [Pr <sub>2</sub> NPO] <sub>4</sub> ( <b>1B</b> )	AA'XX'	[ $\delta_A = \delta_{A'} = 144.4, \delta_X = \delta_{X'} = 63.4$ ] ( $J_{AA'} = J_{XX'} = 50, J_{AX} = J_{A'X'} = 20, J_{AX'} = J_{AX} = 1$ )
PdCl <sub>2</sub> [Pr <sub>2</sub> NPO] <sub>4</sub> ( <b>2A</b> )	A <sub>2</sub> X <sub>2</sub>	[ $\delta_A = 147.8, \delta_X = 88.3$ ] ( $J_{AX} = 44$ )
PdBr <sub>2</sub> [Pr <sub>2</sub> NPO] <sub>4</sub> ( <b>2B</b> )	A <sub>2</sub> X <sub>2</sub>	[ $\delta_A = 146.1, \delta_X = 88.3$ ] ( $J_{AX} = 49$ )
PtCl <sub>2</sub> [Pr <sub>2</sub> NPO] <sub>4</sub> ( <b>3</b> )	A <sub>2</sub> X <sub>2</sub>	[ $\delta_A = 142.8, \delta_X = 59.0$ ] ( $J_{AX} = 34$ )
NiCl <sub>2</sub> [Cy <sub>2</sub> NPO] <sub>4</sub> ( <b>4A</b> )	AA'XX'	[ $\delta_A = \delta_{A'} = 142.3, \delta_X = \delta_{X'} = 54.0$ ] ( $J_{AA'} = J_{XX'} = 50, J_{AX} = J_{A'X'} = 20, J_{AX'} = J_{AX} = 1$ )
NiBr <sub>2</sub> [Cy <sub>2</sub> NPO] <sub>4</sub> ( <b>4B</b> )	AA'XX'	[ $\delta_A = \delta_{A'} = 142.4, \delta_X = \delta_{X'} = 62.3$ ] ( $J_{AA'} = J_{XX'} = 50, J_{AX} = J_{A'X'} = 20, J_{AX'} = J_{AX} = 1$ )
NiI <sub>2</sub> [Cy <sub>2</sub> NPO] <sub>4</sub> ( <b>4C</b> )	AA'XX'	[ $\delta_A = \delta_{A'} = 142.4, \delta_X = \delta_{X'} = 75.4$ ] ( $J_{AA'} = J_{XX'} = 50, J_{AX} = J_{A'X'} = 20, J_{AX'} = J_{AX} = 1$ )
PdCl <sub>2</sub> [Cy <sub>2</sub> NPO] <sub>4</sub> ( <b>5A</b> )	A <sub>2</sub> X <sub>2</sub>	[ $\delta_A = 143.9, \delta_X = 88.9$ ] ( $J_{AX} = 83$ )
PdBr <sub>2</sub> [Cy <sub>2</sub> NPO] <sub>4</sub> ( <b>5B</b> )	A <sub>2</sub> X <sub>2</sub>	[ $\delta_A = 141.9, \delta_X = 88.8$ ] ( $J_{AX} = 88$ )
PtCl <sub>2</sub> [Cy <sub>2</sub> NPO] <sub>4</sub> ( <b>6A</b> )	A <sub>2</sub> X <sub>2</sub>	[ $\delta_A = 146.8, \delta_X = 59.3$ ] ( $J_{AX} = 64, J_{\text{P-P}} = 4826$ )
PtCl <sub>2</sub> [Cy <sub>2</sub> NPO] <sub>4</sub> ( <b>6B</b> )	AMX <sub>2</sub>	[ $\delta_A = 140.1, \delta_M = 134.4, \delta_X = 58.1$ ] ( $J_{AM} \sim 0, J_{AX} = 44, J_{MX} = 13$ )
NiCl <sub>2</sub> [Cy <sub>2</sub> NPO] <sub>5</sub> ( <b>7</b> )	AA'MXX'	[ $\delta_A = \delta_{A'} = 143.9, \delta_M = 124.6, \delta_X = \delta_{X'} = 91.7$ ] ( $J$ 's < 15, poorly resolved)
PdCl <sub>2</sub> [Cy <sub>2</sub> NPO] <sub>5</sub> ( <b>8A</b> )	AA'MXX'	[ $\delta_A = \delta_{A'} = 143.4, \delta_M = 127.5, \delta_X = \delta_{X'} = 87.9$ ] ( $J_{AA'} = J_{XX'} = 50, J_{AX} = J_{A'X'} = 15, J_{AM} = J_{A'M} = 3, J_{MX} = J_{M'X'} = 12$ )
PdBr <sub>2</sub> [Cy <sub>2</sub> NPO] <sub>5</sub> ( <b>8B</b> )	AA'MXX'	[ $\delta_A = \delta_{A'} = 142.7, \delta_M = 127.3, \delta_X = \delta_{X'} = 87.4$ ] ( $J_{AA'} = J_{XX'} = 50, J_{AX} = J_{A'X'} = 19, J_{AM} = J_{A'M} = 3, J_{MX} = J_{M'X'} = 19$ )
PtCl <sub>2</sub> [Cy <sub>2</sub> NPO] <sub>5</sub> ( <b>9</b> )	AA'MXX'	[ $\delta_A = \delta_{A'} = 141.8, \delta_M = 127.5, \delta_X = \delta_{X'} = 60.1$ ] ( $J_{AA'} = J_{XX'} = 50, J_{AM} = J_{A'M} = 3, J_{AX} = J_{A'X'} = 14, J_{MX} = J_{M'X'} = 11, J_{\text{P-P}} = 5206$ )
Mo(CO) <sub>4</sub> [Pr <sub>2</sub> NPO] <sub>3</sub> ( <b>10A</b> )	A <sub>2</sub> X	[ $\delta_A = 138.5, \delta_X = 130.1$ ] ( $J_{AX} = 2$ )
Mo(CO) <sub>4</sub> [Cy <sub>2</sub> NPO] <sub>3</sub> ( <b>10B</b> )	A <sub>2</sub> X	[ $\delta_A = 136.8, \delta_X = 128.2$ ] ( $J_{AX} = 15$ )
Cr(CO) <sub>4</sub> [Cy <sub>2</sub> NPO] <sub>4</sub> ( <b>11a</b> )	A <sub>2</sub> XY	[ $\delta_A = 177.1, \delta_X = 129.4, \delta_Y = 123.4$ ] ( $J_{AX} = 37, J_{AY} = 10, J_{XY} = 3$ )
Cr(CO) <sub>4</sub> [Cy <sub>2</sub> NPO] <sub>4</sub> ( <b>11b</b> )	A <sub>2</sub> X <sub>2</sub>	[ $\delta_A = 174.0, \delta_X = 138.7$ ] ( $J_{AX} = 63$ )
Fe(CO) <sub>3</sub> [Cy <sub>2</sub> NPO] <sub>4</sub> ( <b>12</b> )	A <sub>2</sub> XY	[ $\delta_A = 163.8, \delta_X = 131.6, \delta_Y = 125.6$ ] ( $J_{AX} = 54, J_{AY} = 0.2, J_{XY} \approx 0$ )
Fe(CO) <sub>3</sub> [Pr <sub>2</sub> NPO] <sub>4</sub> ( <b>13</b> )	A <sub>2</sub> X <sub>2</sub>	[ $\delta_A = 160.6, \delta_X = 145.0$ ] ( $J_{AX} = 39$ )
Fe(CO) <sub>4</sub> [Pr <sub>2</sub> NPO] <sub>4</sub> ( <b>14</b> )	AX <sub>2</sub> Y	[ $\delta_A = 152.5, \delta_X = 24.5, \delta = 6.6$ ] ( $J_{AX} = 15, J_{AY} \approx 0, J_{XY} = 187$ )
Cr <sub>2</sub> (CO) <sub>8</sub> [Cy <sub>2</sub> NPO] <sub>4</sub> ( <b>15</b> )	singlet	[ $\delta = 157.8$ ] ( $J_{AB} = 6, J_{BX} = 34, J_{AX} \approx 0$ )
Cr <sub>2</sub> (CO) <sub>7</sub> [Cy <sub>2</sub> NPO] <sub>5</sub> ( <b>16</b> )	A <sub>2</sub> BX <sub>2</sub>	[ $\delta_A = 176.1, \delta_B = 175.1, \delta_X = 155.4$ ] ( $J_{AB} = 2, J_{AX} = 1, J_{BX} = 17, J_{\text{WP}} = 186$ )
W <sub>2</sub> (CO) <sub>7</sub> [Cy <sub>2</sub> NPO] <sub>5</sub> ( <b>17</b> )	A <sub>2</sub> BX <sub>2</sub>	[ $\delta_A = 267.7, \delta_X = 133.2, \delta_Y = 100.1, \delta_Z = 84.2$ ] ( $J_{AX} = J_{AY} = 13, J_{AZ} = 20, J_{XY} = 101, J_{XZ} = 140, J_{YZ} = 33$ )
W <sub>2</sub> (CO) <sub>6</sub> [Cy <sub>2</sub> NPO] <sub>4</sub> ( <b>18</b> )	AXYZ	[ $\delta = 171.1$ ] ( $J_{AX} = 15, J_{AY} \approx 0, J_{XY} = 187$ )
Cr <sub>2</sub> (CO) <sub>8</sub> [DMP-PO] <sub>4</sub> ( <b>19a</b> )	singlet	[ $\delta = 155.4$ ] ( $\delta = 171.1$ )
Cr <sub>2</sub> (CO) <sub>8</sub> [DMP-PO] <sub>4</sub> ( <b>19b</b> )	singlet	[ $\delta = 155.4$ ] ( $\delta = 155.4$ )
Cr <sub>2</sub> (CO) <sub>7</sub> [DMP-PO] <sub>5</sub> ( <b>20</b> )	A <sub>2</sub> BX <sub>2</sub>	[ $\delta_A = 176.1, \delta_B = 175.1, \delta_X = 155.4$ ] ( $J_{AB} = 6, J_{AX} \approx 0, J_{BX} = 42$ )
Cr <sub>2</sub> (CO) <sub>6</sub> [DMP-PO] <sub>6</sub> ( <b>21</b> )	singlet	[ $\delta = 175.5$ ] ( $\delta = 175.5$ )
Mo <sub>2</sub> (CO) <sub>8</sub> [DMP-PO] <sub>4</sub> ( <b>22</b> )	singlet	[ $\delta = 149.6$ ] ( $\delta = 149.6$ )
NiBr <sub>2</sub> [Cy <sub>2</sub> NPO] <sub>4</sub> Mo(CO) <sub>4</sub> ( <b>23</b> )	AA'XX'	[ $\delta_A = \delta_{A'} = 137.9, \delta_X = \delta_{X'} = 60.7$ ] ( $J_{AX} = J_{A'X'} = 15, J_{AX'} = J_{AX} = 12$ )
PtCl <sub>2</sub> [Cy <sub>2</sub> NPO] <sub>5</sub> Mo(CO) <sub>3</sub> ( <b>24</b> )	AMM'XX'	[ $\delta_A = 157.1, \delta_M = 137.5, \delta_X = 88.9$ ] ( $J_{AM} = J_{A'M} = 28.9, J_{AX} = J_{A'X'} = 9.5, J_{MX} = J_{M'X'} = J_{M'X} = J_{MX'} \approx 0$ )
Fe(CO) <sub>3</sub> [Pr <sub>2</sub> NPO] <sub>4</sub> Mo(CO) <sub>4</sub> ( <b>25</b> )	AB <sub>2</sub> X	[ $\delta_A = 163.5, \delta_B = 160.5, \delta_X = 137.4$ ] ( $J_{AB} = 85, J_{AX} \approx 0, J_{BX} = 5$ )
Ni <sub>2</sub> (CO) <sub>4</sub> [Cy <sub>2</sub> NPO] <sub>4</sub> ( <b>26</b> )	singlet	[ $\delta = 133.8$ ] ( $\delta = 133.8$ )

<sup>a</sup> All spectra were run in CDCl<sub>3</sub>.

phosphido resonance ( $\delta +267.8$ ). An analogous Mo<sub>2</sub>(CO)<sub>6</sub>-[Pr<sub>2</sub>NPO]<sub>4</sub> complex containing a phosphido-bridged metal–metal bond and a cleaved P–O linkage has been reported (Figure 4).<sup>3</sup> Diiron nonacarbonyl gave the same Fe(CO)<sub>3</sub>[Cy<sub>2</sub>NPO]<sub>4</sub> (**13**) product as described above from its reaction with [Cy<sub>2</sub>NPO]<sub>3</sub>.

From bis(2,6-dimethylpiperidino)phosphine oxide ((DMP)<sub>2</sub>P(O)H) and Cr(CO)<sub>6</sub> in refluxing toluene we obtained both isomers of Cr<sub>2</sub>(CO)<sub>8</sub>[DMP-PO]<sub>4</sub> (**19a,b**), Cr<sub>2</sub>(CO)<sub>7</sub>[DMP-PO]<sub>5</sub> (**20**) and traces of a white solid with high spectral (Table 1) symmetry that analyzed as Cr(CO)<sub>3</sub>[DMP-PO]<sub>3</sub> (**21**). The X-ray crystal structures of **19a** and **19b** confirmed their being configurational isomers of the Cr<sub>2</sub>P<sub>4</sub>O<sub>4</sub> core. Complex **19a** adopts the familiar adamantanoid cage structure featuring a tetradentate P<sub>4</sub>O<sub>4</sub> ring in a boat–boat form (Figures 5 and 2E). Complex **19b** has the heterocycle in the long chair form serving to link two four-membered CrPOP chelate rings (Figure 6). X-ray crystallography also revealed the symmetrical **21** to be the novel Cr<sub>2</sub>(CO)<sub>6</sub>[DMP-PO]<sub>6</sub> (Figure 7), a cluster structure featuring the heretofore unknown hexaphosphoxane ring. Significantly, quantitative yields of this same product can be obtained from the cage expansion reaction of Cr<sub>2</sub>(CO)<sub>7</sub>[DMP-PO]<sub>5</sub> (**20**) with (DMP)<sub>2</sub>P(O)H in refluxing xylene. By contrast,

molybdenum hexacarbonyl gave the Mo<sub>2</sub>P<sub>4</sub>O<sub>4</sub> cage complex **22** as the only product regardless of reaction conditions.

No tractable products were obtained from Fe<sub>2</sub>(CO)<sub>9</sub> or dihalide precursors of the nickel triad in this type of thermal reaction. Substitution of the bis(amino)phosphine oxides with various phosphoramidites like (R<sub>2</sub>N)-(R'O)P(O)H also failed to produce any alkoxy- or aryloxy-substituted phosphoxane complexes.

**Reactions of Monometallic Phosphoxane Complexes.** The monometallic phosphoxane complexes synthesized above contain additional available phosphorus donor sites. Several heterobimetallic complexes have been prepared using them as metalla-ligands. These include the Mo(CO)<sub>4</sub>[Cy<sub>2</sub>NPO]<sub>4</sub>NiBr<sub>2</sub> complex (**23**), the Mo(CO)<sub>3</sub>[Cy<sub>2</sub>NPO]<sub>5</sub>PdCl<sub>2</sub> complex **24**, and the Mo(CO)<sub>4</sub>[Pr<sub>2</sub>NPO]<sub>4</sub>Fe(CO)<sub>3</sub> complex **25** (Scheme 1). All have been characterized spectrally and by elemental analyses. The Ni/Mo complex **23** can be assigned a basic structure similar to that of complex **19b** (Figure 6) with the P<sub>4</sub>O<sub>4</sub> ring in the long chair conformation and metals coordinating at opposite ends of the heterocycle. Complex **24** should be a Mo/Pd mixed-metal analogue of the Cr<sub>2</sub>P<sub>5</sub>O<sub>5</sub> cage (complex **16**, Figure 2F) structure. Complex **25** exhibited an AB<sub>2</sub>X pattern in its solution <sup>31</sup>P NMR spectrum (Table 1) and numerous bands in its IR carbonyl spectrum (see Experimental Section). A single-

(3) Yang, H. Y.; Wong, E. H.; Jasinski, J. P.; Pozdaniakov, R. Y.; Woudenberg, R. *Organometallics* **1992**, *11*, 1579.

**Table 2.**  $^{13}\text{C}$  NMR Data for the Cyclic Phosphoxane Complexes<sup>a</sup>

compd	assgnt [ $\delta$ , ppm ( <i>J</i> , Hz)]
<b>1B</b>	CH [48.6, 45.1], CH <sub>3</sub> [24.5, 22.9]
<b>2A</b>	CH [47.7, 47.2], CH <sub>3</sub> [23.2, 19.2]
<b>4B</b>	CH [58.1, 53.5], CH <sub>2</sub> [33.3, 33.1, 26.7, 26.4, 26.1, 25.5, 24.8]
<b>7</b>	CH [58.1, 53.8, 52.7], CH <sub>2</sub> [33.4, 32.4, 29.3, 27.1, 26.5, 25.6, 25.4, 24.9, 21.5]
<b>8A</b>	CH [58.5, 53.7, 52.7], CH <sub>2</sub> [37.7, 35.7, 35.2, 33.2, 32.5, 31.5, 29.2, 26.9, 26.3, 25.3, 24.7]
<b>8B</b>	CH [58.5, 54.1, 53.0], CH <sub>2</sub> [37.6, 37.3, 33.4, 33.1, 32.7, 32.4, 29.1, 27.1, 26.4, 25.8, 25.4, 24.8]
<b>9</b>	CH [58.0, 53.6, 52.9], CH <sub>2</sub> [37.8, 37.2, 33.1, 32.5, 29.3, 27.1, 26.4, 25.8, 25.6, 25.4, 24.8]
<b>10A</b>	CH [47.8, 44.5], CH <sub>3</sub> [24.4, 23.6, 23.2]
<b>10B</b>	CH [57.4, 53.7], CH <sub>2</sub> [34.9, 33.7, 34.2, 26.9, 26.6, 26.5, 25.4, 25.1]
<b>11a</b>	CO [226.0, triplet (10), 219.4, triplet (20)], CH [57.4, 53.2, 52.5], CH <sub>2</sub> [33.7, 33.1, 26.8, 25.6]
<b>12</b>	CO [218.1, multiplet], CH [57.8, 53.5 doublet (9); 52.5, doublet (12)] CH <sub>2</sub> [33.5, 33.0, 26.9, 26.8, 26.3, 25.8, 25.7]
<b>13</b>	CO [218.0, multiplet], CH [47.5; 44.4, doublet (15)], CH <sub>3</sub> [24.1, 22.8]
<b>14</b> ( $-10^\circ$ )	CO [215.8, doublet (15); 215.0, doublet (15)] CH [56.9, doublet (11); 48.0, doublet (12); 46.9, doublet (7); 44.6, doublet (27)] CH <sub>3</sub> [26.4, doublet (11); 23.9, 23.5, 23.2, 22.9]
<b>16</b>	CO [229.9, multiplet; 229.1, triplet (14); 224.4, triplet (9); 219.7, triplet (20); 216.7, triplet (20)] CH [58.5, 58.3, 57.5, doublet (10)], CH <sub>2</sub> [36.2, 35.9, 35.3, 34.8, 34.3, 27.3, 27.1, 26.9, 26.7, 25.8, 25.6, 25.2]
<b>17</b>	CO [213.5, 209.8, 203.6, multiplets]; CH [59.0, 58.7, 58.0, doublet (14)], CH <sub>2</sub> [36.0, 35.4, 35.2, 34.8, 34.3, 27.1, 27.0, 26.9, 26.6, 25.7, 25.5, 25.2, 24.8]
<b>18</b>	CO [212.9, 217.6, 210.8, 210.3, 209.8, 206.9, multiplets], CH [57.8, doublet (10); 57.2, doublet (9); 57.5, doublet (8), CH <sub>2</sub> [34.0, 33.9, 33.7, 33.6, 33.4, 31.5, 26.9, 26.6, 26.5, 25.4, 25.3, 24.9, 22.6]
<b>19a</b>	CO [224.1, triplet (9); 217.1, triplet (19)], CH [45.6], CH <sub>2</sub> [30.9, 14.2], CH <sub>3</sub> [23.2]
<b>19b</b>	CO [213.5, 209.8, 203.6, multiplets], CH [47.3, triplet (4); 46.1], CH <sub>2</sub> [31.0, 30.1, 13.6], CH <sub>3</sub> [23.3, 21.7]
<b>20</b>	CO [229.5, multiplet; 228.3, multiplet; 226.4, triplet (11); 219.3, triplet (21); 216.2, triplet (20)]; CH [47.6, triplet (7); 45.8, 45.6, multiplets], CH <sub>2</sub> [31.4, 31.9, 31.1, 30.9, 30.6, 30.5, 14.2, 14.1, 13.9], CH <sub>3</sub> [23.4, 23.0, 22.9, 22.8, 22.5, 22.4]
<b>21</b>	CO [213.5, triplet (15); 206.9, triplet (12)], CH [45.6, triplet (7)], CH <sub>2</sub> [31.0, 14.1], CH <sub>3</sub> [23.0]
<b>22</b>	CO [213.5, triplet (15); 206.9, triplet (12)] CH [45.6, triplet (7)], CH <sub>2</sub> [31.0, 14.1], CH <sub>3</sub> [23.0]
<b>23</b>	CO [215.9, doublet (12); 215.4, doublet (12); 208.7, triplet (8); 207.7, triplet (10)], CH [58.4, 58.2], CH <sub>2</sub> [36.4, 34.2, 33.5, 32.9, 26.4, 25.9, 25.3, 25.1]
<b>24</b>	CO [218.9, doublet of triplets (39, 13); 216.4, doublet of triplets (39, 13)], CH [59.3, 58.2, 57.7], CH <sub>2</sub> [35.8, 35.4, 34.7, 33.3, 27.0, 26.7, 26.1, 25.4, 25.2, 24.9]
<b>25</b>	CO [219.2, triplet (6); 218.8, doublet (9); 216.7, doublet (54); 211.0, doublet of doublets (9, 3); 207.5, quartet (9)], CH [49.2; 47.6, doublet (9); 44.3, doublet (14)], CH <sub>3</sub> [23.4, 23.0, 22.4]
<b>26</b>	CO [198.0, triplet (2)], CH [55.4, triplet (6)], CH <sub>2</sub> [34.2, 26.6, 25.5]

<sup>a</sup> All spectra were run in CDCl<sub>3</sub> at ambient temperature unless otherwise noted.

**Table 3.** Proton NMR Data for the Cyclic Phosphoxane Complexes<sup>a</sup>

compd	assgnt [ $\delta$ , ppm ( <i>J</i> , Hz)]
<b>1B</b>	CH [4.20, multiplets], CH <sub>3</sub> [1.36, 1.32, 1.31, doublets (6.8 Hz)]
<b>2A</b>	CH [3.74, multiplets], CH <sub>3</sub> [1.36, 1.28, doublet (6.7)]
<b>4B</b>	CH [3.8, broad], CH <sub>2</sub> [1.99–0.84, multiplets]
<b>7</b>	CH [3.6, 3.1, 2.9, broad], CH <sub>2</sub> [2.14–1.07, multiplets]
<b>8A</b>	CH [3.52, 3.04, 2.82, broad], CH <sub>2</sub> [2.25–0.88, multiplets]
<b>8B</b>	CH [3.51, 3.17, 2.80, broad], CH <sub>2</sub> [2.26–0.85, multiplets]
<b>9</b>	CH [3.56, 3.06, 2.79, broad], CH <sub>2</sub> [2.19–0.82, multiplets]
<b>10A</b>	CH [3.86, septet (6.9); 3.7, broad], CH <sub>3</sub> [1.32, 1.31, 1.26, doublets (6.9)]
<b>10B</b>	CH [3.25, broad], CH <sub>2</sub> [1.70–1.18, multiplets]
<b>11a</b>	CH [3.48, broad], CH <sub>2</sub> [1.76–0.84, multiplets]
<b>12</b>	CH [3.52, broad], CH <sub>2</sub> [1.82–0.84, multiplets]
<b>13</b>	CH [3.92, 3.79, broad], CH <sub>3</sub> [1.26, doublet (23)]
<b>14</b> ( $-10^\circ$ )	CH [4.58, 4.15, 3.50, 3.33], CH <sub>3</sub> [1.35, 1.31, 1.24, 1.19, doublets (6)]
<b>16</b>	CH [4.19, 3.76, 3.51, multiplets], CH <sub>2</sub> [1.98–0.84, multiplets]
<b>17</b>	CH [4.21, 3.73, 3.10, multiplets], CH <sub>2</sub> [1.92–0.84, multiplets]
<b>18</b>	CH [3.41, 3.30, 3.20, multiplets], CH <sub>2</sub> [2.03–0.84, multiplets]
<b>19a</b>	CH [4.46], CH <sub>2</sub> [1.15–1.18, multiplets], CH <sub>3</sub> [1.35, doublet (7)]
<b>19b</b>	CH [4.46, 4.22, multiplets], CH <sub>2</sub> [1.87–1.55, multiplets], CH <sub>3</sub> [1.35, 1.40, doublets (7)]
<b>20</b>	CH [4.55, 4.46, 4.37, 4.25, 4.13, multiplets], CH <sub>2</sub> [1.87–1.55, multiplets], CH <sub>3</sub> [1.41, 1.37, 1.32, doublets (7)]
<b>21</b>	CH [4.47, multiplet], CH <sub>2</sub> [1.51–1.19, multiplets], CH <sub>3</sub> [1.37, doublet (7)]
<b>22</b>	CH [4.40, multiplet], CH <sub>2</sub> [1.92–1.50, multiplets], CH <sub>3</sub> [1.31, doublet (7)]
<b>23</b>	CH [3.98, multiplet; 3.8, broad], CH <sub>3</sub> [1.95–0.84, multiplets]
<b>24</b>	CH [4.11, 3.66, multiplets; 3.0, broad], CH <sub>3</sub> [2.06–1.00, multiplets]
<b>25</b>	CH [4.03, 3.87, septets (7); 3.63, broad], CH <sub>3</sub> [1.44, 1.38, 1.33, 1.19, doublets (7)]
<b>26</b>	CH [3.38, broad], CH <sub>2</sub> [2.18–0.72, multiplets]

<sup>a</sup> All spectra were run at ambient temperature in CDCl<sub>3</sub> unless noted otherwise.

crystal X-ray analysis revealed an  $\eta^3\text{-P}_4\text{O}_4$  ring bridging the two metals with an iron–molybdenum bond completing pseudooctahedral coordination spheres at both metals (Figure 8).

In attempts to prepare heterobimetallic complexes of the nickel triad, phosphoxane ring transfer reactions were observed instead. For example, PdBr<sub>2</sub> and PtCl<sub>2</sub> were found to displace the 1,3-chelated NiBr<sub>2</sub> from

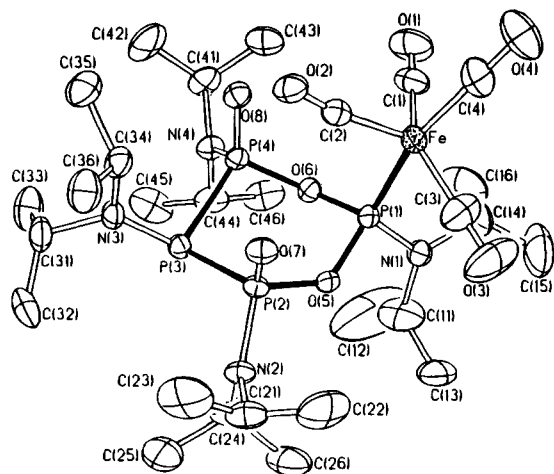


Figure 3. Molecular structure of  $\text{Fe}(\text{CO})_4[\text{1Pr}_2\text{NPO}]_4$  (14).

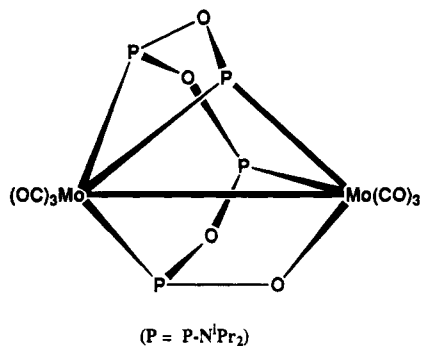


Figure 4. Molecular structure of  $\text{Mo}_2(\text{CO})_6[\text{1Pr}_2\text{NPO}]_4$ .<sup>3</sup>

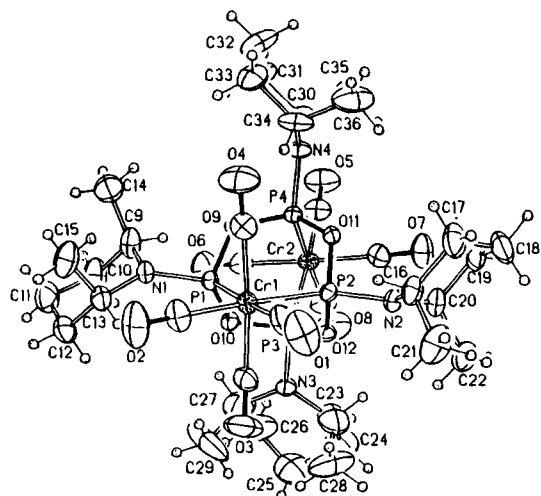


Figure 5. Molecular structure of  $\text{Cr}_2(\text{CO})_6[\text{DMP-PO}]_4$  (19a).

complex **4B** to give the respective 1,5- $\text{P}_4\text{O}_4$  complexes (**5B**, **6**) at room temperature (Scheme 2). At lower temperature, an intermediate 1,3-chelated  $\text{PtCl}_2$  complex (Figure 2B) can be identified by  $^{31}\text{P}$  NMR spectroscopy (AA'XX' pattern).

A reductive decarbonylation occurred in the thermal reactions of either  $\text{Fe}(\text{CO})_5$  or  $\text{Fe}_2(\text{CO})_9$  with  $\text{NiBr}_2[\text{Cy}_2\text{NPO}]_4$  (**4B**) in attempts to prepare a Ni/Fe complex. The only isolated phosphoxane product was identified as  $\text{Ni}_2(\text{CO})_4[\text{Cy}_2\text{NPO}]_4$  complex **26**, a nickel analogue of adamantanoid cages like **19a** (see Figures 2E and 5).

**X-Ray Structural Studies. (1) Molecular Structure of  $\text{Fe}(\text{CO})_4[\text{1Pr}_2\text{NPO}]_4$  (14).** The coordination geometry around iron is essentially trigonal bipyramidal

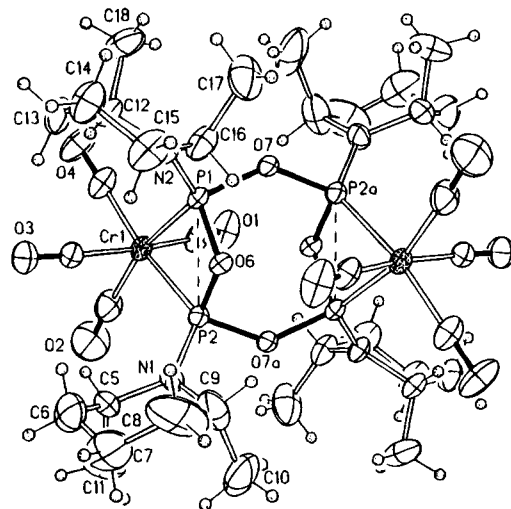


Figure 6. Molecular structure of  $\text{Cr}_2(\text{CO})_8[\text{DMP-PO}]_4$  (19b).

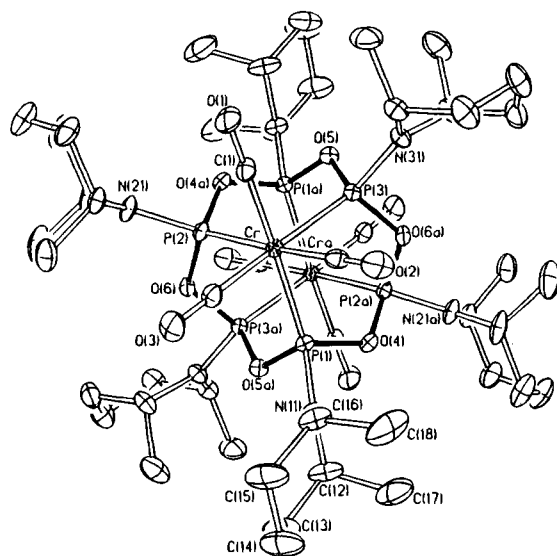
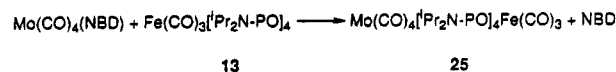
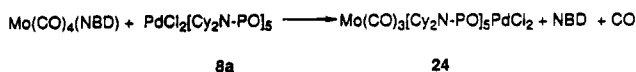
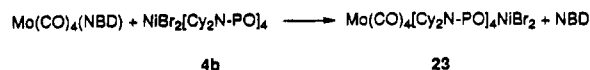


Figure 7. Molecular structure of  $\text{Cr}_2(\text{CO})_6[\text{DMP-PO}]_6$  (21).

#### Scheme 1



with the lone phosphorus donor in one axial site (Figure 3). An Fe–P bond length of 2.189(2) Å is toward the short side of typical values for phosphine– $\text{Fe}(\text{CO})_4$  structures (2.22–2.37 Å).<sup>4</sup> The axial Fe–C(4) bond is at 1.763(10) Å. The diaxial P(1)–Fe–C(4) angle is considerably bent from linearity at 161.3(2)°. While the equatorial coordination plane is well defined by Fe, C(1), C(2), and C(3), the C(1)–Fe–C(3) angle has opened up

(4) Riley, P. E.; Davis, R. E. *Inorg. Chem.* **1980**, *19*, 159. Massimbeni, L. R. *Inorg. Nucl. Chem. Lett.* **1971**, *7*, 187. Wong, E. H.; Bradley, F. C.; Prasad, L.; Gabe, E. J. *J. Organomet. Chem.* **1984**, *263*, 167. Pickardt, J.; Rosch, L.; Schumann, H. *J. Organomet. Chem.* **1976**, *107*, 241. Kilbourn, B. T.; Raeburn, U. A.; Thompson, D. T. *J. Chem. Soc. A* **1969**, 1906. Einstein, F. W. B.; Jones, R. D. G. *J. Chem. Soc., Dalton Trans.* **1972**, 442.

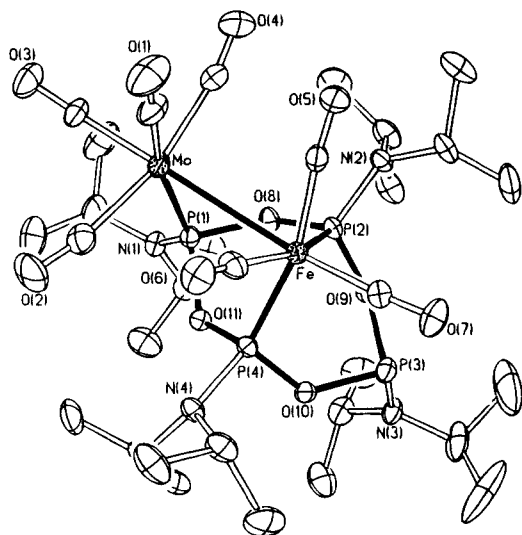


**Figure 8.** Molecular structure of  $\text{Fe}(\text{CO})_3[\text{iPr}_2\text{NPO}]_4\text{Mo}(\text{CO})_4$  (**25**).

**Scheme 2**

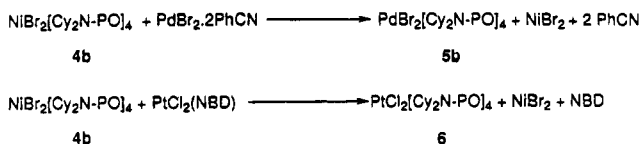


**Table 4.** Selected Bond Distances and Angles for Complex **14**

Bond Distances (Å)			
Fe–P(1)	2.189(2)	Fe–C(1)	1.775(7)
Fe–C(2)	1.821(5)	Fe–C(3)	1.776(9)
Fe–C(4)	1.763(10)	P(1)–O(5)	1.627(3)
P(1)–O(6)	1.636(4)	P(1)–N(1)	1.644(4)
P(2)–P(3)	2.234(2)	P(2)–O(5)	1.641(3)
P(2)–O(7)	1.451(4)	P(2)–N(2)	1.640(4)
P(3)–P(4)	2.227(2)	P(3)–N(3)	1.673(4)
P(4)–O(6)	1.628(3)	P(4)–O(8)	1.456(4)
P(4)–N(4)	1.640(5)	O(1)–C(1)	1.145(9)
O(2)–C(2)	1.131(6)	O(3)–C(3)	1.139(11)
O(4)–C(4)	1.149(13)		

Bond Angles (deg)			
P(1)–Fe–P(1)	87.5(3)	P(1)–Fe–C(2)	101.6(2)
C(1)–Fe–C(2)	105.4(3)	P(1)–Fe–C(3)	84.9(3)
C(1)–Fe–C(3)	144.5(3)	C(2)–Fe–C(3)	110.2(3)
P(1)–Fe–C(4)	161.3(2)	Fe–O(1)–O(6)	115.9(1)
C(2)–Fe–C(4)	97.1(3)	C(1)–Fe–C(4)	87.3(4)
Fe–P(1)–O(5)	118.0(1)	C(3)–Fe–C(4)	88.9(4)
O(5)–P(1)–O(6)	98.3(2)	P(3)–P(2)–O(7)	116.7(2)
P(3)–P(2)–O(5)	102.2(1)	P(3)–P(4)–O(6)	101.1(1)
O(5)–P(2)–O(7)	112.6(2)	O(6)–P(4)–O(8)	113.8(2)
P(2)–P(3)–P(4)	99.3(1)	P(1)–O(5)–P(2)	130.1(2)
P(3)–P(4)–O(8)	116.5(1)	Fe–C(1)–O(1)	179.1(7)
P(1)–O(6)–P(4)	131.0(2)	Fe–C(3)–P(3)	179.3(6)
Fe–C(2)–O(2)	172.1(6)		
Fe–C(4)–O(4)	179.5(8)		

to an unusually large  $144.5(3)^\circ$  at the expense of the other two  $\text{C}(\text{eq})\text{--Fe--C}(\text{eq})$  angles ( $105.4(3)^\circ$  and  $110.2(5)^\circ$ ). One of the  $\text{Fe--C}$  distances ( $\text{Fe--C}(2)$ ) is significantly elongated to  $1.821(5)$  Å compared to the other two equatorial bonds at  $1.775(7)$  and  $1.776(9)$  Å. This particular carbonyl group also tilts away from the two axial ring phosphoryl oxygens, resulting in an obtuse  $\text{P}(1)\text{--Fe--C}(2)$  angle of  $101.6(2)^\circ$  and  $\text{C}(2)\text{--Fe--C}(4)$  angle of  $97.1(3)^\circ$ . Selected bond distances and angles are listed in Table 4.

A chair conformation of the  $\text{P}_4\text{O}_2$  heterocycle is observed with all four diisopropylamino groups in

**Table 5.** Selected Bond Distances and Angles for Complex **19a**

Bond Distances (Å)			
Cr(1)–P(1)	2.329(2)	Cr(1)–P(2)	2.340(2)
Cr(1)–C(1)	1.872(7)	Cr(1)–C(2)	1.851(6)
Cr(1)–C(3)	1.879(6)	Cr(1)–C(4)	1.895(6)
Cr(2)–P(3)	2.323(2)	Cr(2)–P(4)	2.337(2)
Cr(2)–C(5)	1.864(6)	Cr(2)–C(6)	1.892(6)
Cr(2)–C(7)	1.886(6)	Cr(2)–C(8)	1.856(6)
P(1)–N(1)	1.643(4)	P(1)–O(9)	1.631(3)
P(1)–O(10)	1.662(3)	P(2)–O(12)	1.656(3)
P(2)–O(12)	1.646(3)	P(2)–N(2)	1.632(4)
P(3)–N(3)	1.638(4)	P(3)–O(10)	1.647(3)
P(3)–O(12)	1.638(3)	P(4)–N(4)	1.632(4)
P(4)–O(9)	1.661(3)	P(4)–O(11)	1.644(3)
O(1)–C(1)	1.135(8)	O(2)–C(2)	1.148(8)
O(3)–C(3)	1.137(8)	O(4)–C(4)	1.136(7)
O(5)–C(5)	1.152(7)	O(6)–C(6)	1.130(7)
O(7)–C(7)	1.140(8)	O(8)–C(8)	1.140(7)

Bond Angles (deg)			
P(1)–Cr(1)–P(2)	80.0(1)	P(1)–Cr(1)–C(1)	177.3(2)
P(2)–Cr(1)–C(1)	97.6(2)	P(1)–Cr(1)–C(2)	98.0(2)
P(2)–Cr(1)–C(2)	176.1(2)	C(1)–Cr(1)–C(2)	84.5(3)
P(1)–Cr(1)–C(3)	93.5(2)	P(2)–Cr(1)–C(3)	90.6(2)
C(1)–Cr(1)–C(3)	87.7(3)	C(2)–Cr(1)–C(3)	86.1(3)
P(1)–Cr(1)–C(4)	90.9(2)	P(2)–Cr(1)–C(4)	95.4(2)
C(1)–Cr(1)–C(4)	88.1(3)	C(2)–Cr(1)–C(4)	88.0(3)
C(3)–Cr(1)–C(4)	173.1(3)	P(3)–Cr(2)–P(4)	79.4(1)
P(3)–Cr(2)–C(5)	175.2(2)	P(4)–Cr(2)–C(5)	100.8(2)
P(3)–Cr(2)–C(6)	88.7(2)	P(4)–Cr(2)–C(6)	97.3(2)
C(5)–Cr(2)–C(6)	86.6(3)	P(3)–Cr(2)–C(6)	98.6(2)
P(4)–Cr(2)–C(7)	88.5(2)	C(5)–Cr(2)–C(7)	86.2(3)
C(6)–Cr(2)–C(7)	171.4(3)	P(3)–Cr(2)–C(8)	92.7(2)
P(4)–Cr(2)–C(8)	170.6(2)	C(5)–Cr(2)–C(8)	87.5(3)
C(6)–Cr(2)–C(8)	87.5(3)	C(7)–Cr(2)–C(8)	87.6(3)
O(9)–P(1)–O(10)	99.5(2)	O(11)–P(2)–O(12)	98.8(2)
O(10)–P(3)–O(12)	101.4(2)	O(9)–P(4)–O(11)	98.3(2)
P(1)–O(9)–P(4)	128.4(2)	P(1)–O(10)–P(3)	127.6(2)
P(2)–O(11)–P(4)	129.6(2)	P(2)–O(12)–O(3)	126.5(2)

equatorial positions and the two phosphoryl oxygens axial. Ring phosphorus–phosphorus bond distances of  $2.234(2)$  and  $2.227(2)$  Å are comparable to known  $\text{P--P} (= \text{O})$  bond lengths.<sup>5</sup>

**(2) Molecular Structure of  $\text{Cr}_2(\text{CO})_8[\text{DMP-PO}]_4$  (19a).** The basic  $\text{M}_2\text{P}_4\text{O}_4$  adamantanoid cage structure (Figure 2E) is adopted in the solid-state structure of complex **19a** (Figure 5). A boat–boat conformation of the core tetraphosphoxane ring enables it to chelate two chromium vertices in a back-to-back mode. Ring  $\text{P--O}$  distances range from  $1.631(3)$  to  $1.662(3)$  Å while  $\text{P--O--P}$  angles vary slightly from  $126.6(2)^\circ$  to  $128.4(2)^\circ$ . The four ring oxygens are planar to within  $0.039$  Å. Deviations from octahedral bond angles at the chromiums include the not-quite-linear axial carbonyls at  $171.4(3)\text{--}173.1(2)^\circ$ , the compressed  $\text{P--Cr--P}$  angles at  $79.4(1)^\circ$  and  $80.0(1)^\circ$ , and *trans*-carbonyl– $\text{Cr--P}$  angles from  $84.5(3)^\circ$  to  $87.5(3)^\circ$ . Metal–phosphorus distances vary only slightly from  $2.323(2)$  to  $2.340(2)$  Å and axial carbonyl–metal distances ( $1.879(6)\text{--}1.895(6)$  Å) are indeed slightly longer than equatorial ones ( $1.851(6)\text{--}1.872(6)$  Å) as expected. The intracage  $\text{Cr--Cr}$  separation is at  $5.656(1)$  Å. Other selected bond distances and angles are listed in Table 5.

**(3) Molecular Structure of  $\text{Cr}_2(\text{CO})_8[\text{DMP-PO}]_4$  (19b).** The molecule has an inversion center with the tetraphosphoxane  $\text{P}_4\text{O}_4$  ring conformation best described as a long chair with  $\text{O}(6)$  and  $\text{O}(6a)$  forming the back

(5) Weber, D.; Fluck, E.; Von Schnering, H. G.; Peters, K. Z. *Naturforsch., B: Anorg. Chem., Org. Chem.* **1982**, *37B*, 594, 1580. Turnbull, M. M.; Wong, E. H.; Gabe, E. J.; Lee, F. L. *Inorg. Chem.* **1986**, *25*, 3189.

**Table 6.** Selected Bond Distances and Angles for Complex 19b

Bond Distances (Å)			
Cr(1)–P(1)	2.337(1)	Cr(1)–P(2)	2.333(1)
Cr(1)–C(1)	1.884(4)	Cr(1)–C(2)	1.862(6)
Cr(1)–C(3)	1.875(4)	Cr(1)–C(4)	1.872(5)
P(1)–P(2)	2.560(1)	P(1)–N(2)	1.633(3)
P(1)–O(1)	1.657(3)	P(1)–O(7)	1.635(3)
P(2)–N(1)	1.627(4)	P(2)–O(6)	1.664(3)
P(2)–O(7A)	1.630(2)	O(1)–C(1)	1.152(5)
O(2)–C(2)	1.144(8)	O(3)–C(3)	1.141(5)
O(4)–C(4)	1.141(6)	O(7)–P(2A)	1.630(2)

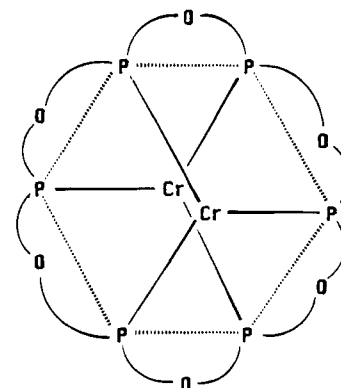
  

Bond Angles (deg)			
P(1)–Cr(1)–P(2)	66.5(1)	P(1)–Cr(1)–C(1)	97.9(2)
P(2)–Cr(1)–C(1)	98.7(2)	P(1)–Cr(1)–C(2)	162.7(2)
P(2)–Cr(1)–C(2)	96.3(2)	C(1)–Cr(1)–C(2)	85.5(2)
P(1)–Cr(1)–C(3)	89.9(2)	P(2)–Cr(1)–C(3)	91.3(2)
C(1)–Cr(1)–C(3)	169.2(2)	C(2)–Cr(1)–C(3)	89.3(2)
P(1)–Cr(1)–C(4)	100.2(2)	P(2)–Cr(1)–C(4)	166.4(2)
C(1)–Cr(1)–C(4)	85.6(4)	C(2)–Cr(1)–C(4)	96.9(2)
C(3)–Cr(1)–C(4)	85.6(2)	O(6)–P(2)–O(7A)	98.8(1)
P(1)–O(6)–P(2)	100.9(2)	P(1)–O(7)–P(2A)	134.5(2)

and leg and P(1), P(2), O(7a), P(1a), P(2a), and O(7) the planar seat (Figure 6). Significantly longer P–O bonds of 1.660(4) Å are observed in the strained chelate rings compared to those in the rest of the ring (1.632(4) Å). Also, the compressed P(1)–O(6)–P(2) angle of 100.9(2)° in the four-membered chelate rings can be contrasted with the much larger 134.5(2)° found for the remaining P–O–P angles. Transannular P(1)–P(2) separations are at only 2.560(1) Å. Two Cr(CO)<sub>4</sub> groups are coordinated to opposite sides of this heterocycle by four-membered chelate rings to give approximately octahedral environments at the metals. Bending of the axial carbonyls away from the phosphoxane ring is observed with a C(1)–Cr(1)–C(3) angle of 169.2(2)°. The cramped P(1)–Cr(1)–P(2) and P(1)–O(6)–P(2) angles of 66.5(1)° and 100.9(2)°, respectively have precedence in related chromium phosphoxane chelate rings.<sup>2,6</sup> Metal–phosphorus distances at 2.333(1) and 2.337(1) Å are unexceptional. Selected bond distances and angles are listed in Table 6. Interestingly, the two methyl substituents in each of the dimethylpiperidino groups adopt diaxial positions with the piperidino nitrogens effectively planar.

**(4) Molecular Structure of Cr<sub>2</sub>(CO)<sub>6</sub>[DMP-PO]<sub>6</sub> (21).** The centrosymmetric core structure of the hexaphosphoxane complex 21 (Figure 7) features two *fac*-Cr(CO)<sub>3</sub>, six phosphorus, and six oxygen vertices. A novel P<sub>6</sub>O<sub>6</sub> macrocycle serves as a hexadentate donor toward two metal centers, one above and one below. This can also be viewed as a Cr<sub>2</sub>P<sub>6</sub> cube with oxygens bridging only the P–P edges (Figure 9). Cage phosphoxane P–O–P angles range from 123.3(3)° to 124.8(2)°. Bond angles around the metals are reasonably close to orthogonal values with P–Cr–P angles ranging from 92.7(1)° to 93.0(1)° and C–Cr–C angles from 88.0(3)° to 90.2(3)°. Average Cr–P bond lengths of 2.335(2) Å and Cr–C distances of 1.857(6) Å are found. The intracage Cr–Cr separation is down to 4.700(1) Å. Other selected bond distances and angles are listed in Table 7.

**(5) Molecular Structure of Fe(CO)<sub>3</sub>[<sup>1</sup>Pr<sub>2</sub>NPO]<sub>4</sub>Mo(CO)<sub>4</sub> (25).** This heterobimetallic complex contains a

**Figure 9.** Schematic view of the Cr<sub>2</sub>P<sub>6</sub>O<sub>6</sub> core in complex 21.**Table 7.** Selected Bond Distances and Angles for Complex 21

Bond Distances (Å)			
Cr–P(1)	2.325(1)	Cr–P(2)	2.325(1)
Cr–P(3)	2.321(1)	Cr–C(1)	1.866(5)
Cr–C(2)	1.857(5)	Cr–C(3)	1.860(4)
P(1)–O(4)	1.647(2)	P(1)–N(11)	1.649(4)
P(1)–O(5A)	1.638(3)	P(2)–O(6)	1.648(3)
P(2)–N(21)	1.645(4)	P(2)–O(4A)	1.639(3)
P(3)–O(6A)	1.641(3)	O(1)–C(1)	1.145(6)
O(2)–C(2)	1.152(6)	O(3)–C(3)	1.145(5)
O(4)–P(2A)	1.639(3)	O(5)–P(1A)	1.638(3)
O(6)–P(3A)	1.641(3)		

Bond Angles (deg)			
P(1)–Cr–P(2)	92.8(1)	P(1)–Cr–P(3)	93.1(1)
P(2)–Cr–P(3)	93.0(1)	P(1)–Cr–C(1)	177.1(1)
P(2)–Cr–C(1)	87.0(1)	P(3)–Cr–C(1)	89.8(1)
P(1)–Cr–C(2)	90.0(1)	P(2)–Cr–C(2)	177.2(1)
P(3)–Cr–C(2)	87.0(1)	C(1)–Cr–C(2)	90.2(2)
P(1)–Cr–C(3)	87.0(1)	P(2)–Cr–C(3)	89.7(1)
P(3)–Cr–C(3)	177.3(1)	C(1)–Cr–C(3)	90.1(2)
P(2)–Cr–C(3)	90.3(2)	O(4)–P(1)–O(5A)	97.0(1)
O(6)–P(2)–O(4A)	96.8(1)	O(5)–P(3)–O(6A)	96.8(1)
P(1)–O(4)–P(2A)	123.7(2)	P(3)–O(5)–P(1A)	123.7(2)
P(2)–O(6)–P(3A)	123.7(1)		

metal-bridging tridentate P<sub>4</sub>O<sub>4</sub> ring in a chair–chair conformation (Figure 8). In addition to the often observed 1,5-chelating coordination mode toward Fe (Figure 2A), a third phosphorus is also ligating to the Mo(CO)<sub>4</sub> fragment. A long Fe–Mo bond of 3.034(2) Å completes the pseudooctahedral coordination sphere at each metal. At Mo, an acute Fe–Mo–P(1) angle of 72.9(1)° is found while all four carbonyls are pushed away from the FeP<sub>4</sub>O<sub>4</sub> unit with Fe–Mo–C and P(1)–Mo–C angles ranging from 93.7(2)° to as much as 102.1(2)° (P(1)–Mo–C(3)). The Mo–C(3) bond *trans* to the Fe is the shortest at 1.946(8) Å while those *cis* to both the Fe and P(1) are longest at 2.036(8)–2.057(8) Å. A Mo–P(1) bond of 2.473(2) Å can also be noted. At the Fe center, the two carbonyls *trans* to the phosphorus atoms are bent toward the Mo(CO)<sub>4</sub> moiety with Mo–Fe–C(5) and Mo–Fe–C(6) angles of only 71.8(3)° and 73.7(2)°, respectively, while that *trans* to the Mo is bent away from the P<sub>4</sub>O<sub>4</sub> ring with the P–Fe–C(7) angle at about 100°. The two Fe–P distances are at 2.218(2) and 2.225(2) Å. Other selected bond distances and angles are listed in Table 8.

The tetraphosphoxane ring itself retains the approximate chair–chair conformation as was found for complex 2A.<sup>2</sup> Interestingly, two ranges of P–O bond lengths are observed. Those at the chelating P(2) and

(6) Wong, E. H.; Prasad, L.; Gabe, E. J.; Bradley, F. C. J. *Organomet. Chem.* 1982, 236, 321.

**Table 8.** Selected Distances and Angles for Complex **25**

Bond Distances (Å)			
Mo-Fe	3.034(2)	Mo-P(1)	2.473(2)
Mo-C(1)	1.984(6)	Mo-C(2)	2.057(8)
Mo-C(3)	1.946(8)	Mo-C(4)	2.036(8)
Fe-P(2)	2.225(2)	Fe-P(4)	2.218(2)
Fe-C(5)	1.796(7)	Fe-C(6)	1.798(7)
Fe-C(7)	1.792(7)	P(1)-O(8)	1.663(4)
P(1)-O(11)	1.669(5)	P(2)-O(8)	1.621(4)
P(2)-O(9)	1.621(5)	P(3)-O(9)	1.675(6)
P(3)-O(10)	1.658(4)	P(4)-O(10)	1.621(5)
P(4)-O(11)	1.622(4)	O(1)-C(1)	1.152(8)
O(2)-C(2)	1.124(9)	O(3)-C(3)	1.152(10)
O(4)-C(4)	1.139(11)	O(5)-C(5)	1.142(8)
O(6)-C(6)	1.143(8)	O(7)-C(7)	1.138(9)
Bond Angles (deg)			
Fe-Mo-P(1)	72.9(1)	Fe-Mo-C(1)	94.8(2)
P(1)-Mo-C(1)	167.6(2)	Fe-Mo-C(2)	97.5(3)
P(1)-Mo-C(2)	96.0(2)	C(1)-Mo-C(2)	86.8(3)
Fe-Mo-C(3)	174.7(2)	P(1)-Mo-C(3)	102.1(2)
C(1)-Mo-C(3)	90.1(3)	C(2)-Mo-C(3)	84.5(3)
Fe-Mo-C(4)	95.0(3)	P(1)-Mo-C(4)	93.7(2)
C(1)-Mo-C(4)	85.9(3)	C(2)-Mo-C(4)	166.0(4)
C(3)-Mo-C(4)	83.6(3)	Mo-Fe-P(2)	89.8(1)
Mo-Fe-P(4)	90.4(1)	P(2)-Fe-P(4)	83.0(1)
Mo-Fe-C(5)	73.7(2)	P(2)-Fe-C(5)	91.9(2)
P(4)-Fe-C(5)	163.4(2)	Mo-Fe-C(6)	71.8(3)
P(2)-Fe-C(6)	160.5(2)	P(4)-Fe-C(6)	90.6(2)
C(5)-Fe-C(6)	89.0(3)	Mo-Fe-C(7)	166.2(2)
P(2)-Fe-C(7)	100.1(2)	P(4)-Fe-C(7)	100.2(2)
C(5)-Fe-C(7)	96.3(3)	C(6)-Fe-C(7)	99.2(3)
Mo-P(1)-O(8)	109.5(1)	Mo-P(1)-O(11)	112.3(1)
O(8)-P(1)-O(11)	97.9(2)	Fe-P(2)-O(8)	112.4(2)
Fe-P(2)-O(9)	113.5(2)	O(8)-P(2)-O(9)	97.7(2)
O(9)-P(2)-O(10)	96.1(2)	Fe-P(4)-O(10)	113.0(1)
Fe-P(4)-O(11)	111.1(2)	O(10)-P(4)-O(11)	99.9(2)
P(1)-O(8)-P(2)	117.7(2)	P(2)-O(9)-P(3)	127.0(2)
P(3)-O(10)-P(4)	127.4(2)	P(1)-O(11)-P(4)	119.5(2)
Mo-C(1)-O(1)	178.4(7)	Mo-C(2)-O(2)	171.4(8)
Mo-C(3)-O(3)	178.2(5)	Mo-C(4)-O(4)	170.2(8)
Fe-C(5)-O(5)	172.9(6)	Fe-C(6)-O(6)	171.6(6)
Fe-C(7)-O(7)	174.8(5)		

P(4) are all around 1.621(5) Å while the remainders are significantly longer, varying from 1.658(4) to 1.675(6) Å.

## Discussion

**Formation of the Cyclic Phosphoxane Complexes.** The variety of products obtained from preformed triphosphoxane rings [R<sub>2</sub>NPO]<sub>3</sub> (R = <sup>i</sup>Pr, Cy) with nickel, palladium, or platinum dihalides illustrates some of the subtle and still not well-understood factors that influenced the reaction course. Though diisopropylamino and dicyclohexylamino substituents would not be expected to differ dramatically in their stereoelectronic influences,<sup>7</sup> [<sup>i</sup>Pr<sub>2</sub>NPO]<sub>3</sub> yielded only P<sub>4</sub>O<sub>4</sub> complexes while [Cy<sub>2</sub>NPO]<sub>3</sub> led to both P<sub>4</sub>O<sub>4</sub> and P<sub>5</sub>O<sub>5</sub> products. There is a general pattern in higher reaction temperatures favoring formation of the larger P<sub>5</sub>O<sub>5</sub> rings except in the nickel dichloride case. The nature of the ancillary halides in NiX<sub>2</sub> (X = Cl, Br, I) also made a difference. Of the three, only NiCl<sub>2</sub> yielded a P<sub>5</sub>O<sub>5</sub> complex.

The 1,3-coordination mode (Figure 2B) in the NiP<sub>4</sub>O<sub>4</sub> (Figures 4A-C and 7) products as revealed by a characteristic AA'XX' <sup>31</sup>P NMR spectrum was unique to the nickel dihalides, presumably due to a superior fit in the resulting four-membered NiPOP chelate ring. Although the actual conformation of the tetraphosphox-

ane ring itself has not been determined, its ability to further coordinate a second metal to give Mo(CO)<sub>4</sub>[Cy<sub>2</sub>NPO]<sub>4</sub>NiBr<sub>2</sub> (**23**) suggests the long chair form with the opposite side of the ring available for coordination of a second metal (Figures 2B and 6). The X-ray structure of Cr(CO)<sub>4</sub>[DMP-PO]<sub>4</sub>Cr(CO)<sub>4</sub> (**19b**, Figure 6) lends credence to this premise. Observation of well-resolved NMR resonances for all the isolated NiX<sub>2</sub> phosphoxane complexes (**1A,B**, **4A-C**, **7**, **23**) is consistent with near-square-planar nickel coordination geometries and diamagnetism in all these cases.

The assembly of P<sub>4</sub>O<sub>4</sub> and P<sub>5</sub>O<sub>5</sub> complexes from cyclic triphosphoxane under reaction conditions as mild as 4° requires exclusive head-to-tail grafting in of extra R<sub>2</sub>-NP=O phosphinidene units. Existence of such intermediates has been substantiated by several previous reports.<sup>8</sup> It is very likely that prior metal coordination represents an essential prerequisite to these ring expansions. It is also noteworthy that we failed to isolate any products incorporating more than one divalent metal center regardless of the reaction stoichiometry. Subsequent studies indeed revealed the reluctance of divalent metal MP<sub>n</sub>O<sub>n</sub> complexes to coordinate a second divalent metal center even though zero-valent metals were readily bound. Electronic effects transmitted through the P-O-P linkages may be responsible for this selectivity. We have recently reported on such intramolecular influences in a series of heterobimetallic P<sub>4</sub>O<sub>4</sub> cage complexes.<sup>9,10</sup> Cage complexes containing two Mo<sup>II</sup> vertices can be synthesized indirectly from halogenation reactions of Mo<sup>0</sup>P<sub>4</sub>O<sub>4</sub>Mo<sup>0</sup> precursors.<sup>14</sup>

Under similar reaction conditions, Fe<sub>2</sub>(CO)<sub>9</sub> gave significantly different products, depending on the cyclic triphosphoxane used. While [Cy<sub>2</sub>NPO]<sub>3</sub> yielded Fe(CO)<sub>3</sub>[Cy<sub>2</sub>NPO]<sub>4</sub> (**12**) with an 1,5-η<sup>2</sup>-P<sub>4</sub>O<sub>4</sub> ring in a boat-chair configuration (Figure 2C), [<sup>i</sup>Pr<sub>2</sub>NPO]<sub>3</sub> produced instead Fe(CO)<sub>3</sub>[<sup>i</sup>Pr<sub>2</sub>NPO]<sub>4</sub> (**13**), the chair-chair (Figure 2A) isomer, and a novel Fe(CO)<sub>4</sub>-η<sup>1</sup>-([<sup>i</sup>Pr<sub>2</sub>NPO]<sub>4</sub>) complex (**14**). The X-ray structure of the latter (Figure 3) revealed coordination of a Fe(CO)<sub>4</sub> fragment to a P[OP(=O)]<sub>2</sub>P ring. This unusual six-membered ring can be viewed as the product of a double P-O-P to P-P(=O) rearrangement, converting a tetraphosphoxane η<sup>1</sup>-P<sub>4</sub>O<sub>4</sub> ring into a mondentate P[OP(=O)]<sub>2</sub>P heterocycle. It is conceivable that the eight-membered P<sub>4</sub>O<sub>4</sub> ring was initially formed but was unstable toward such a rearrangement to a six-membered ring with two strong phosphoryl P=O bonds. We have previously reported a single P-O-P to P-P(=O) rearrangement in the metallocycle *cis*-M(CO)<sub>4</sub>(PPh<sub>2</sub>O)<sub>2</sub>PPh to form *cis*-M(CO)<sub>4</sub>[PPh<sub>2</sub>P(O)PhOPPh<sub>2</sub>] (M = Cr, Mo, W).<sup>11a</sup>

Three diaminophosphine oxides, (R<sub>2</sub>N)<sub>2</sub>P(O)H (R<sub>2</sub>N = <sup>i</sup>Pr<sub>2</sub>N, Cy<sub>2</sub>N, DMP), were used as sources of R<sub>2</sub>NP=O phosphinidene oxide units in thermal reactions with group 6 metal carbonyls. All three have in common

(8) Niecke, E.; Engelmann, M.; Zorn, H.; Krebs, B.; Henkel, G. *Angew. Chem., Int. Ed. Engl.* **1990**, *19*, 710. Chasar, D. W.; Fackler, J. P.; Mazany, A. M.; Komoroski, R. A.; Kroenke, W. J. *J. Am. Chem. Soc.* **1986**, *108*, 5956. Quast, H.; Heuschmann, M. *Angew. Chem., Int. Ed. Engl.* **1978**, *17*, 867.

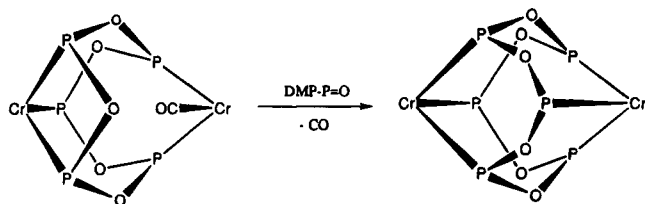
(9) Yang, H. Y.; Wong, E. H.; Rheingold, A. L.; Owens-Waltermire, B. E. *J. Chem. Soc., Chem. Commun.* **1993**, 35.

(10) Yang, H. Y.; Wong, E. H.; Rheingold, A. L.; Waltermire, B. E. *Organometallics*, in press.

(11) (a) Wong, E. H.; Bradley, F. C.; Gabe, E. J. *J. Organomet. Chem.* **1983**, *244*, 235. (b) Bader, D. S.; Turnbull, M. M. *Polyhedron* **1990**, *9*, 2619.

(7) Seligson, A. L.; Trogler, W. C. *J. Am. Chem. Soc.* **1991**, *113*, 2520.

Scheme 3



amino substituents with secondary  $\alpha$ -carbons. We have previously found that less bulky dialkylamino groups like Et<sub>2</sub>N failed to lead to P<sub>n</sub>O<sub>n</sub> products under these conditions.<sup>2</sup> Presumably the dialkylamine elimination critical to the generation of R<sub>2</sub>NP=O units from (R<sub>2</sub>N)<sub>2</sub>P(O)H is only viable with the bulkier R groups. A correlation between the steric bulk of the dialkylamino substituents and success of cage formation from dialkylamino phosphine oxides has been made.<sup>11b</sup>

Again, the size and coordination mode of the P<sub>n</sub>O<sub>n</sub> rings formed in the complexes isolated were sensitive to the nature of both precursors and the reaction conditions. In general, only P<sub>3</sub>O<sub>3</sub> and P<sub>4</sub>O<sub>4</sub> complexes were formed around the Mo(CO)<sub>4</sub> moiety. Although a lone Mo<sub>2</sub>(CO)<sub>6</sub>[Me-AsO]<sub>6</sub> structure has been reported previously,<sup>12</sup> no Mo<sub>2</sub>P<sub>6</sub>O<sub>6</sub> species was isolated here in our studies. It may be that the smaller P<sub>6</sub>O<sub>6</sub> core cannot accommodate two *fac*-Mo(CO)<sub>3</sub> vertices. By contrast, in addition to two isomers of the Cr<sub>2</sub>P<sub>4</sub>O<sub>4</sub> cores (19a,b), larger ring P<sub>5</sub>O<sub>5</sub> and P<sub>6</sub>O<sub>6</sub> products were also isolated around Cr(CO)<sub>n</sub> (*n* = 3, 4) fragments. Further, among the products isolated, only chromium formed stable four-membered MPOP chelate rings (complexes 16 and 19b), the shorter Cr–P bond apparently resulting in less strained ring geometries. Larger cages incorporating Cr(CO)<sub>3</sub> vertices are increasingly favored with higher reaction temperatures. Conceivably, progressive assembly of P<sub>3</sub>O<sub>3</sub> to P<sub>4</sub>O<sub>4</sub> to P<sub>5</sub>O<sub>5</sub> to P<sub>6</sub>O<sub>6</sub> rings about the metal carbonyl centers as more CO's are lost underlie the syntheses of these products. This is not unexpected since the loss of a third carbonyl from the Cr(CO)<sub>4</sub> center should be possible only under more forcing conditions.<sup>13</sup> Indeed, it is tempting upon examining the related structures of the Cr<sub>2</sub>P<sub>5</sub>O<sub>5</sub> (20) and Cr<sub>2</sub>P<sub>6</sub>O<sub>6</sub> (21) cores to speculate on the loss of a third CO from the *cis*-Cr(CO)<sub>4</sub> vertex in 20 with incorporation of an extra phosphinidene oxide unit (Scheme 3) to build up to the hexaphosphoxane complex 21. This speculation was amply supported by the quantitative conversion of 20 to 21 upon refluxing in xylene in the presence of extra (DMP)<sub>2</sub>P(O)H as the phosphinidene oxide source.

**Metal Coordination Reactions of Monometallic Cyclic Phosphoxane Complexes.** Heterobimetallic complexes were accessible from the monometallic polyphosphoxane complexes since they have phosphorus lone pairs available. Isolated complexes include Mo(CO)<sub>4</sub>[Cy<sub>2</sub>NPO]<sub>4</sub>NiBr<sub>2</sub> (23), Mo(CO)<sub>3</sub>[Cy<sub>2</sub>NPO]<sub>5</sub>PdCl<sub>2</sub> (24), and Mo(CO)<sub>4</sub>[<sup>i</sup>Pr<sub>2</sub>NPO]<sub>4</sub>Fe(CO)<sub>3</sub> (25) (Scheme 1). The first two have parallels in known M<sub>2</sub>P<sub>n</sub>O<sub>n</sub> structures. Complex 23 can be assigned a long chair ring conformation based on its <sup>31</sup>P NMR spectrum (Table 1), at its core a configurational isomer of the previously

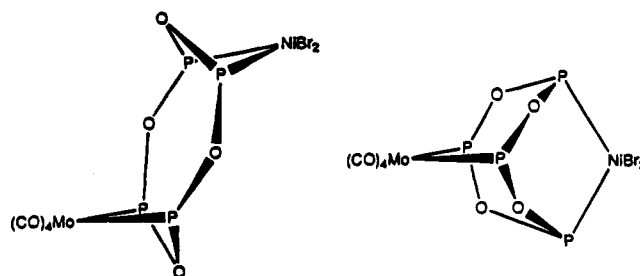


**Figure 10.** Two core geometries of Mo(CO)<sub>4</sub>[R<sub>2</sub>NPO]<sub>4</sub>NiBr<sub>2</sub> (P = R<sub>2</sub>NP).

reported Mo(CO)<sub>4</sub>[<sup>i</sup>Pr<sub>2</sub>NPO]<sub>4</sub>NiBr<sub>2</sub> cage complex (Figure 10).<sup>9,10</sup> Interestingly, the latter is paramagnetic and has been found to have a pseudotetrahedral geometry at the Ni center.<sup>9</sup> We ascribe these different nickel coordination geometries to steric factors engendered by the positioning of the cage dialkylamino groups, which disfavors a square-planar Ni coordination geometry. Complex 24 is a Pd/Mo analogue of the Cr<sub>2</sub>P<sub>5</sub>O<sub>5</sub> cage core (complexes 16 and 20, Figure 2F). Its ready formation from PdCl<sub>2</sub>[Cy<sub>2</sub>NPO]<sub>5</sub> (8A) supports the <sup>31</sup>P NMR-based geometry of the precursor (Figure 2G). The unique complex 25 was found to have an η<sup>3</sup>-P<sub>4</sub>O<sub>4</sub> ring bridging the two metal centers. Furthermore, EAN electron counting would be consistent with a dative iron to molybdenum bond, completing pseudo-octahedral environments at both sites.

Again, no bimetallic products containing two divalent metal vertices were isolated. This confirms the reluctance of such P<sub>n</sub>O<sub>n</sub> rings to incorporate two relatively electron-demanding centers. The only such complexes we know of are the tetrahalogenated molybdenum cage species Mo(CO)<sub>2</sub>X<sub>2</sub>[RPO]<sub>4</sub>Mo(CO)<sub>2</sub>X<sub>2</sub> (X = Cl, Br, I; R = <sup>i</sup>Pr<sub>2</sub>N, Ph) prepared from direct halogenations of the parent cages. Even these rare exceptions were found to be relatively less tractable species.<sup>14</sup>

Attempts at synthesizing Ni/Pd and Ni/Pt complexes revealed instead phosphoxane ring transfer reactions whereby the P<sub>n</sub>O<sub>n</sub> heterocycle was displaced from NiBr<sub>2</sub>[Cy<sub>2</sub>NPO]<sub>4</sub> (4B) by the heavier metals to form the more stable 1,5-chelates (5B, 6). Previously, we reported a pyridine displacement of the [<sup>i</sup>Pr<sub>2</sub>NPO]<sub>4</sub> tetraphosphoxane free ligand from its NiBr<sub>2</sub> complex at –30 °C.<sup>2</sup> Similar displacements failed with the palladium complexes. Observation of the PtCl<sub>2</sub>-1,3-[Cy<sub>2</sub>NPO]<sub>4</sub> intermediate at low temperature (<sup>31</sup>P NMR, AA'XX' pattern) suggested that the transfer reaction may proceed via a bimetallic intermediate followed by loss of nickel and a subsequent 1,3- to 1,5-rearrangement of the chelation mode (Scheme 4).

Reductive carbonylation of the NiBr<sub>2</sub> vertex in the reactions of complex 4B with Fe(CO)<sub>5</sub> and Fe<sub>2</sub>(CO)<sub>9</sub> to give Ni<sub>2</sub>(CO)<sub>4</sub>[Cy<sub>2</sub>NPO]<sub>4</sub> (26) has precedence in the reported use of iron carbonyls as both reducing and carbonylating agents toward metal dihalides.<sup>15</sup> The initially formed Ni(CO)<sub>2</sub>[Cy<sub>2</sub>NPO]<sub>4</sub> then can dimerize with loss of four phosphinidene oxide units to form the cage complex 26.

**<sup>31</sup>P NMR Spectroscopy of the Cyclic Phosphoxane Complexes.** <sup>31</sup>P NMR spectroscopy remains the

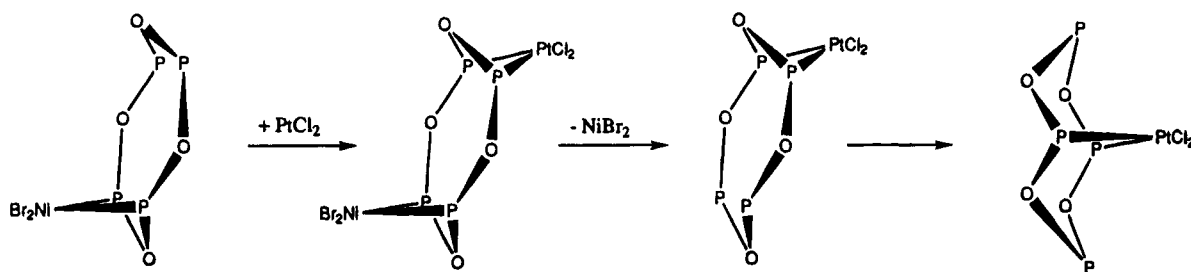
(12) Rheingold, A. L. *Organometallics* 1986, 5, 393.

(13) Kirtly, S. W. *Comprehensive Organometallic Chemistry*; Wilkinson, G., Stone, F. G. A., Abel, E. W., Eds.; Pergamon Press: New York, 1982; Vol. 3.

(14) Turnbull, M. M.; Valdez, C.; Wong, E. H.; Gabe, E. J.; Lee, F. L. *Inorg. Chem.* 1992, 31, 208.

(15) Booth, B. L.; Else, M. J.; Fields, R.; Goldwhile, H.; Hazeldine, R. N. *J. Organomet. Chem.* 1968, 14, 417. Nesmeynov, A. N.; Isaeva, L. S.; Morozova, L. N. *Inorg. Chim. Acta* 1978, 29, L210.

Scheme 4



single most powerful tool for structural determination of the described cyclic phosphoxane complexes in solution. The well-known dependence of  ${}^2J_{PP}$  on lone pair orientation has proven to be useful for structural assignments in a variety of polyphosphorus compounds.<sup>16</sup> In the known cyclic phosphoxane complexes, magnitudes of observed  ${}^2J_{POP}$  range from less than 1 to over 60 Hz, with lone pairs *syn* to the coordinated metals accounting for most of the larger values. For example, in the chair–chair form (Figure 11A) of  $MP_4O_4$  ( $M = Cr, Mo, W, Fe, Pd, Pt$ ) possessing *syn* lone pairs,  ${}^2J_{POP}$  were observed at 28–88 Hz. For the chair–boat form (Figure 11B) ( $M = Cr, Mo, W, Fe, Pt$ ), the *syn* values range from 38 to 59 Hz while the *anti* couplings are significantly smaller at 1–13 Hz. In the lone boat–boat complex  $Mo(CO)_4[Pr_2NPO]_4$  (Figure 11C) with both lone pairs *anti* to the coordinated metal,  ${}^2J_{POP}$  is 2 Hz only.<sup>9,10</sup> We also noted that high-temperature (to 100 °C) spectral studies failed to reveal any interconversions between these isomeric structures (Figure 11A–C), thus confirming typically high phosphorus inversion barriers. These coupling data also allowed us to propose solution structures of several  $MP_5O_5$  complexes with some confidence. For example,  $PdX_2P_5O_5$  (**8A**, **8B**) and  $PtCl_2P_5O_5$  (**9**) are assigned structures (Figure 11D) on the basis of their AA'MXX' spectral patterns, their small  ${}^2J_{AX}$  and  ${}^2J_{MX}$  of 11–19 Hz, and the actual observation of  ${}^4J_{AM}$ 's of about 3 Hz in each case. The ready formation of the  $MoP_5O_5Pd$  (**24**, Figure 2F) cage complex from **8A** lends further support for these structural designations.

The well-known “ring effect” or ring contribution ( $\Delta_R$ ) to the  ${}^{31}P$  chemical shifts of four- to six-membered phosphine chelates has been recently ascribed by Lindner to originate from the component of the shift tensor perpendicular to the ring plane.<sup>17–19</sup> For our complexes, it proved very helpful in identifying the existence of four-membered chelate rings. For example, the four-membered  $CrPOP$  chelate rings in complex **19b** ( $\delta$  155.4) can be distinguished from the six-membered rings in the adamantanoid cage structure of **19a** ( $\delta$  171.1) by their upfield shift. This effect also manifested itself in the mixed-metal complex **23**, where the relatively upfield shift ( $\delta$  137.9) of the  $Mo$ -bounded  $P$ 's compared to typical larger chelate ring values ( $\delta \sim 150$ ) is fully consistent with formation of four-membered chelates rings using the long chair form of  $P_4O_4$  (Figure

**2B**). Similarly, the 1,3-coordination mode of the  $NiX_2P_4O_4$  complexes can be gauged from their upfield  $\delta$ 's of 54–63. Nickel analogues of the 1,5-chelated  $PdX_2P_4O_4$  structure would be expected to have chemical shifts downfield from the 88 ppm region.<sup>17</sup> Thus, the  $NiP_5O_5$  complex was assigned its structure (Figures 2G and 11D) partly on the basis of this downfield  $\delta$  value of 91.7 observed for its coordinated  $P$ 's, invalidating the presence of any four-membered chelate rings.

Bridging phosphido and phosphoryl units in these complexes are readily identified by their unique chemical shifts at very low and high fields, respectively, compared to typical  $P(NR_2)(OR')_2$  centers whose shifts range from  $\delta +60$  to  $+180$ .<sup>16,20</sup> Finally, complexes **10A** and **10B** both contain a  $P_3O_3$  ring which can be either in a boat or in a chair form. We favor the chair form (Figure 2D) in both cases since the upfield shift of the lone uncoordinated  $P_x$  from  $\delta$  140.3 to 130.1 and 128.2, respectively, upon complex formation should be a result of the parent triphosphoxane flipping into a chair form. This will remove the transannular  $P=O$  interaction present in the parent boat-form heterocycle and lead to the observed upfield shift.

Room-temperature  ${}^{13}C$  NMR studies of the iron  $FeP_4O_4$  complex **14** in  $CDCl_3$  revealed fluxional carbonyls resulting in observation of a single doublet resonance at  $\delta +215.8$  ( ${}^2J_{CP} = 15$  Hz). Interestingly, in addition to the usual sharp signals, both the methyl ( $\delta$ 's 26.4 and 23.1) and methine ( $\delta$ 's 56.9, 44.9) regions exhibited two broad resonances at room temperature which sharpened into doublets at  $-10$  °C. In toluene- $d_8$  at about 100 °C, these coalesced to broad singlets at around  $\delta$  25 and  $\delta$  51. Decomposition precluded observation of spectra at the fast-exchange regime. We ascribe these changes to a hindered rotation around the  $P-NiPr_2$  bond at the iron-coordinating phosphorus center since the solid-state structure (Figure 3) showed a significant bending back of the  $Fe(CO)_4$  unit away from the two axial phosphoryl oxygens and toward this particular diisopropylamino group.

**X-Ray Structures of Cyclic Phosphoxane Complexes.** The highly distorted equatorial  $C(1)-Fe-C(3)$  angle of  $144.5(3)^\circ$  in the structure of complex **14** may be traced to two origins. One of the  $P(1)-N(1)$ -diisopropyl groups is oriented so that a methine  $C(14)-H$  is pointed directly into the region between  $C(1)$  and  $C(3)$  (Figure 3). Concurrently, a tilting away of the equatorial iron coordination plane at  $C(2)$  ( $C(2)-Fe-P(1)$  angle of  $101.6(2)^\circ$ ) from the two axial ring phosphoryl oxygens toward this methine group may also contribute to the opening up of this angle. As a consequence of this, an elongated  $Fe-C(2)$  bond ( $1.821(5)$  Å) also results while

(16) Verkade, J. G.; Quin, L. D., Eds. *Phosphorus-31 NMR Spectroscopy in Stereochemical Analysis: Organic Compounds and Metal Complexes*; VCH Publishers: Deerfield Beach, FL, 1987.

(17) Garrou, P. E. *Chem. Rev.* **1981**, *81*, 229.

(18) Lindner, E.; Fawzi, R.; Mayer, H. A.; Eichele, K.; Hiller, W. *Organometallics* **1992**, *11*, 1033.

(19) Pregosin, P. S.; Kunz, R. W.  *${}^{31}P$  and  ${}^{13}C$  NMR of Transition Metal Phosphine Complexes*; Springer-Verlag: New York, 1979.

(20) Gorenstein, D. G.  *${}^{31}P$  NMR*; Academic Press: New York, 1984.

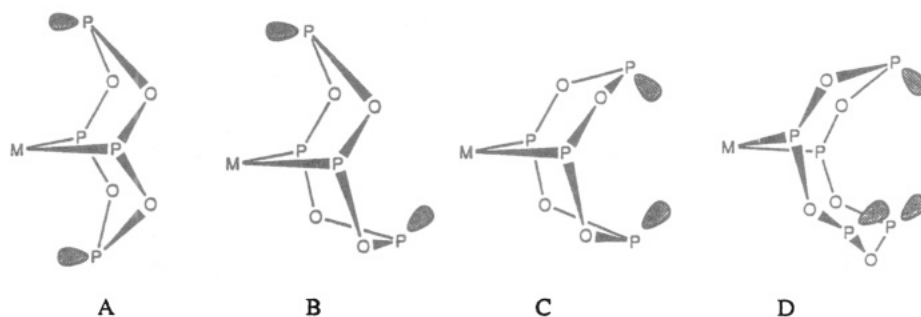


**Figure 11.** *Syn* and *anti* phosphorus lone pairs in  $MP_4O_4$  and  $MP_5O_5$  ( $P = R_2NP$ ).

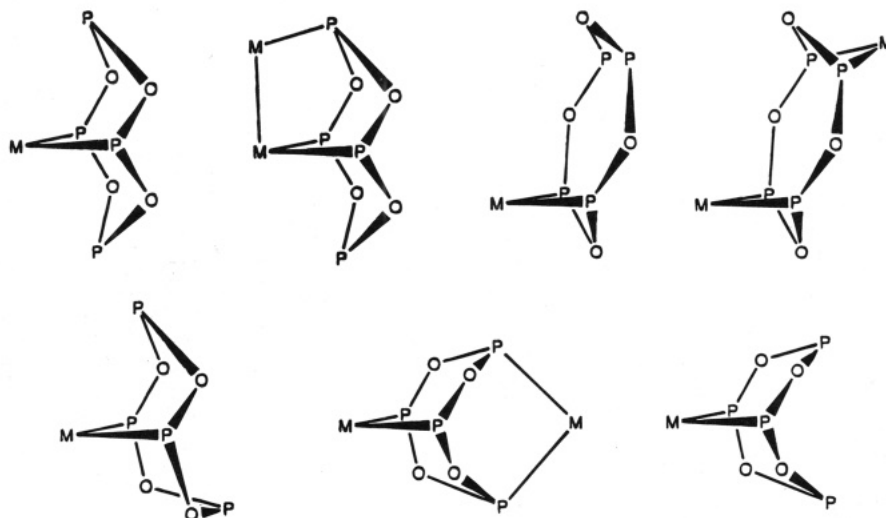


**Figure 12.** Known coordination modes of the  $P_4O_4$  tetraphosphoxane heterocycle ( $P = R_2NP$ ).

the remaining Fe–C distances are quite similar to each other (1.76–1.78 Å).

Comparison to the original  $Mo_2P_4O_4$  geometry reveals the slightly more compact  $Cr_2P_4O_4$  core in complex **19a** with shorter average Cr–P distances of 2.332(3) Å compared to 2.501(2) Å in the former.<sup>21</sup> Average cage P–O–P angles are also less in **19a** (128.0(3)°) than in the molybdenum cage (131.0(2)°). Further, the intracage Cr–Cr separation is down to 5.656(1) Å from the Mo–Mo value of 6.001(1) Å. The deviations from idealized octahedral geometry about the metal center are also less in the dichromium cage structure. For example, the axial carbonyls subtend an angle of 172° at Cr and 167° at Mo while the P–M–P angles are 79.7(2)° and 75.96(5)°, respectively, indicative of the better fit of the more compact chromium vertices.

Aside from the distinct coordination modes and conformations of the  $\eta^4$ - $P_4O_4$  ring, comparison of structural details between the **19a** cage and its long chair configurational isomer **19b** revealed only a few dramatic differences. The presence of two strained four-membered CrPOP chelate rings in the latter resulted in two types of wildly differing P–O–P angles of 100.9(2)° and 134.5(2)°. These smaller chelate rings enforced a P–Cr–P angle of 66.5(1)° and a wider C(eq)–Cr–C(eq) angle of 96.9(2)° than similar values in the cage structure of 80° and around 86°, respectively. In spite of these, no significant variations in Cr–P, Cr–C, or P–O distances were found.

The lone precedent for the  $M_2P_6O_6$  core geometry of complex **21** (Figures 7 and 9) is the  $Mo_2(CO)_6[Me-AsO]_6$  complex formed in the reaction of  $Mo(CO)_6$  with  $[Me-AsO]_5$  in the presence of air.<sup>12</sup> A description of the latter

structure as a flattened  $As_6O_6$  cubooctahedron *trans*-capped by  $Mo(CO)_3$  units can also describe the geometry of **21**. The longer As–O distances apparently allowed accommodation of two *fac*- $Mo(CO)_3$  vertices while only smaller  $Cr(CO)_3$  units are incorporated into the hexaphosphoxane core. This superior fit can be seen in the nearly ideal octahedral angles observed at the chromium centers with all their structural details closely mirroring those reported for the acyclic *fac*- $Cr(CO)_3$ -( $PH_3$ )<sub>3</sub>.<sup>22</sup> The considerable decrease of intracage Cr–Cr distance from the  $Cr_2P_4O_4$  cage value of 5.656(1) to 4.700(1) Å in the  $Cr_2P_6O_6$  cage reflects a flattening of the  $P_6O_6$  core. Consistent with this observation, slightly smaller phosphoxane P–O–P angles of around 124° are observed compared to that of 128° in the  $Cr_2P_4O_4$  cage.

All three structures featuring the dimethylpiperidino substituent (**19a**, **19b**, **21**) revealed diaxial positioning of their 2,6-dimethyls. Adoption of this normally unfavored conformation is presumably due to the near-planarity at their ring nitrogens and a similar preference for axial methyls in substituted piperidines containing *N*-nitroso, *N*-acetyl, and *N*-nitro groups.<sup>23</sup>

The novel tridentate coordination geometry of the  $P_4O_4$  ring in the iron–molybdenum complex **25** extends to seven the known ligating modes of the versatile tetraphosphoxane ligand (Figure 12). The long Fe–Mo bond of 3.034(2) Å has ample precedence in known Fe/

(21) Wong, E. H.; Turnbull, M. M.; Hutchinson, K. D.; Valdez, C.; Gabe, E. J.; Lee, F. L.; LePage, Y. *J. Am. Chem. Soc.* **1988**, *110*, 8422.

(22) Huttner, G.; Schelle, S. *J. Organomet. Chem.* **1973**, *47*, 383.

(23) Fraser, R. R.; Grindley, C. *J. Chem.* **1975**, *53*, 2465. Ripperger, H. *Z. Chem.* **1977**, *17*, 177.

Mo cluster compounds, and its presence ensures the electron-precise nature of the complex.<sup>24</sup> In accord with this dative Fe → Mo bonding, a distinctly strengthened and shorter Mo–C(3) bond *trans* to this interaction of 1.946(8) Å is observed compared to the other Mo–C bonds which range from 1.98 to 2.06 Å.

### Experimental Section

All manipulations were carried out using standard Schlenk techniques under an atmosphere of prepurified nitrogen. Hexane was distilled from CaH<sub>2</sub> and toluene from sodium, while THF was distilled from sodium benzophenone ketyl. Triethylamine was distilled from KOH before use. Phosphorus trichloride, diisopropylamine, dicyclohexylamine, dimethylpiperidine, and xylene were reagent grade chemicals obtained from Aldrich Chemicals. Group 6 metal hexacarbonyls and iron carbonyls were purchased from Pressure Chemicals, Inc. Norbornadiene chromium tetracarbonyl,<sup>25</sup> (NBD)Mo(CO)<sub>4</sub>,<sup>26</sup> (NBD)W(CO)<sub>4</sub>,<sup>27</sup> (cycloheptatriene)Mo(CO)<sub>3</sub>,<sup>28</sup> NiCl<sub>2</sub>·DME, NiBr<sub>2</sub>·DME,<sup>29</sup> NiI<sub>2</sub>·2THF,<sup>30</sup> PdCl<sub>2</sub>(PhCN)<sub>2</sub>,<sup>31</sup> PdBr<sub>2</sub>(PhCN)<sub>2</sub>,<sup>32</sup> and (NBD)PtCl<sub>2</sub><sup>33</sup> were all prepared according to literature methods. The phosphine oxides (Pr<sub>2</sub>N)<sub>2</sub>P(O)H and (Cy<sub>2</sub>N)<sub>2</sub>P(O)H and the triphosphoxane [Pr<sub>2</sub>NPO]<sub>3</sub> were prepared as described previously.<sup>2</sup>

Proton, <sup>13</sup>C{<sup>1</sup>H}, <sup>31</sup>P{<sup>1</sup>H} NMR spectra were recorded on JEOL FX90Q and Bruker AM 360 spectrometers using internal deuterium lock. Proton and <sup>13</sup>C chemical shifts were referenced to internal TMS while <sup>31</sup>P shifts were referenced to external 85% phosphoric acid. Infrared spectra were recorded on a Perkin-Elmer 283B instrument using KBr pellets. Elemental analyses were performed at the University of New Hampshire Instrumentation Center with a Perkin-Elmer 2400 elemental analyzer.

**NiCl<sub>2</sub>[Pr<sub>2</sub>NPO]<sub>4</sub> (1A) and NiBr<sub>2</sub>[Pr<sub>2</sub>NPO]<sub>4</sub> (1B).** The synthesis and elemental analyses of complex **1B** have been described in ref 2. A similar procedure was used to prepare **1A**: A 2.0 g (4.5 mmol) amount of [Pr<sub>2</sub>NPO]<sub>3</sub> and 0.60 g (2.7 mmol) of NiCl<sub>2</sub>·DME were stirred in 30 mL of hexane for 24 h. The yellow suspension turned brown and was filtered, and the residue was washed with hexane. After dissolution of the brown solid in CH<sub>2</sub>Cl<sub>2</sub> and filtration through Celite to remove residual NiCl<sub>2</sub>·DME, the filtrate was evaporated to dryness to give crude **1A** as a brown powder (0.80 g, 44% based on Ni). Although a satisfactory <sup>31</sup>P NMR spectrum was obtained (Table 1), acceptable elemental analyses were not available due to its low stability. IR, ν<sub>POP</sub> 939 cm<sup>-1</sup>.

**PdCl<sub>2</sub>[Pr<sub>2</sub>NPO]<sub>4</sub> (2A) and PdBr<sub>2</sub>[Pr<sub>2</sub>NPO]<sub>4</sub> (2B).** The synthesis and spectral and structural characterization of **2A** were described in ref 2. A similar procedure was used to prepare **2B**: Triphosphoxane [Pr<sub>2</sub>NPO]<sub>3</sub> (0.30 g, 0.68 mmol) and 0.20 g (0.42 mmol) of PdBr<sub>2</sub>·2PhCN were refluxed in 30 mL of hexane for 6 h. The orange suspension turned yellow and after cooling to room temperature was filtered to give a light yellow residue. This was washed with hexane and dried

under reduced pressure to give 0.41 g (40% based on Pd) of **2B**: IR, ν<sub>POP</sub> 896 cm<sup>-1</sup>. Anal. Calcd for C<sub>24</sub>H<sub>66</sub>Br<sub>2</sub>N<sub>4</sub>O<sub>4</sub>P<sub>4</sub>Pd: N, 6.60; C, 33.71; H, 6.60. Found: N, 6.46; C, 34.12; H, 6.77.

**PtCl<sub>2</sub>[Pr<sub>2</sub>NPO]<sub>4</sub> (3).** The triphosphoxane (0.30 g, 0.68 mmol) and 0.15 g (0.42 mmol) of (NBD)PtCl<sub>2</sub> were refluxed in 20 mL of hexane for 6 h. After cooling to room temperature, the white residue was filtered off, washed with hexane, and dried to give 0.27 g (75% based on Pt) of crude **3**. Attempts to further purify this white powder were not successful.

**[Cy<sub>2</sub>NPO]<sub>3</sub>.** The triphosphoxane was prepared from Cy<sub>2</sub>-NPCL<sub>2</sub> as follows: An amount of 27.5 g (87.0 mmol) of Cy<sub>2</sub>-NPCL<sub>2</sub> and 27.0 mL (194 mmol) of triethylamine in 100 mL of THF were chilled in an ice bath. From a dropping funnel, 30 mL of the THF containing 1.70 mL (94.0 mmol) of water was added dropwise over 2 h with rigorous stirring of the reaction mixture. After complete addition, the mixture was allowed to warm to room temperature and then heated to reflux for about 1 h. The thick white precipitate of amine hydrochloride was filtered off and the filtrate evaporated to dryness under reduced pressure. The white residue resulting was then extracted with hot hexane and filtered. Upon cooling, a white solid precipitated which was filtered and dried to give 33 g (56%) of the pure triphosphoxane: IR, ν<sub>POP</sub> 820, 846 cm<sup>-1</sup>. Anal. Calcd for C<sub>36</sub>H<sub>66</sub>N<sub>3</sub>O<sub>3</sub>P<sub>3</sub>: N, 6.16; C, 63.43; H, 9.69. Found: N, 6.29; C, 63.23; H, 9.75.

**NiCl<sub>2</sub>[Cy<sub>2</sub>NPO]<sub>4</sub> (4B).** A 6.2 g (9.1 mmol) amount of triphosphoxane and 1.0 g (4.6 mmol) of NiCl<sub>2</sub>·DME were stirred in 30 mL of hot toluene at 90 °C. After 5 h, the initially yellow suspension became red. Cooling, filtration, and evaporation of the filtrate gave 2.4 g (50% based on Ni) of crude **4A**. This unstable red powder gave satisfactory NMR data but could not be further purified due to ready decomposition.

**NiBr<sub>2</sub>[Cy<sub>2</sub>NPO]<sub>4</sub> (4B).** Triphosphoxane (1.7 g, 2.5 mmol) and NiBr<sub>2</sub>·DME (0.56 g, 1.8 mmol) were stirred in 30 mL of hexane for 24 h. The orange-red suspension turned brown. After filtration and washing with hexane, the residue was dissolved in CH<sub>2</sub>Cl<sub>2</sub> and filtered through Celite to give 1.2 g (60% based on Ni) of orange **4B**: IR, ν<sub>POP</sub> 932 cm<sup>-1</sup>. Anal. Calcd for C<sub>48</sub>H<sub>88</sub>Br<sub>2</sub>N<sub>4</sub>NiO<sub>4</sub>P<sub>4</sub>: N, 4.96; C, 51.12; H, 7.86. Found: N, 4.75, C, 50.93; H, 8.18.

**NiI<sub>2</sub>[Cy<sub>2</sub>NPO]<sub>4</sub> (4C).** A 0.60 g (0.90 mmol) amount of the triphosphoxane and 0.18 g (0.39 mmol) of NiI<sub>2</sub>·2THF were stirred in 30 mL of THF. After 3 h, the purple suspension turned red-purple and was filtered through Celite. The filtrate was evaporated to dryness, washed by hexane, and dried under reduced pressure to give unstable **4C** as a red-purple powder.

**PdCl<sub>2</sub>[Cy<sub>2</sub>NPO]<sub>4</sub> (5A).** Triphosphoxane (1.1 g, 1.6 mmol) and PdCl<sub>2</sub>·2PhCN (0.46 g, 1.2 mmol) were stirred in 30 mL of hexane at 4 °C in the cold room. After 72 h, the orange suspension turned yellow. Filtration, washing with hexane, and drying gave a yellow powder (1.0 g, 77% based on Pd) of crude **5A** which was not further purified: IR, ν<sub>POP</sub> 880 cm<sup>-1</sup>.

**PdBr<sub>2</sub>[Cy<sub>2</sub>NPO]<sub>4</sub> (5B).** Triphosphoxane (1.1 g, 1.6 mmol) and PdBr<sub>2</sub>·2PhCN (0.50 g, 1.1 mmol) were stirred at 4 °C in 30 mL of hexane. After 72 h, the yellow suspension was filtered, and the residue was washed with hexane and dried under reduced pressure to give 0.91 g (70% based on Pd) of complex **5B**: IR, ν<sub>POP</sub> 878 cm<sup>-1</sup>. Anal. Calcd for C<sub>48</sub>H<sub>88</sub>Br<sub>2</sub>N<sub>4</sub>O<sub>4</sub>P<sub>4</sub>Pd: N, 4.77; C, 49.05; H, 7.55. Found: N, 4.61; C, 49.34; H, 7.70.

**PtCl<sub>2</sub>[Cy<sub>2</sub>NPO]<sub>4</sub> (6).** Triphosphoxane (0.44 g, 0.64 mmol) and 0.15 g (0.40 mmol) of PtCl<sub>2</sub>(NBD) were stirred at 4 °C in 20 mL of hexane for 72 h. The white suspension was filtered and dried to give a white solid. Solution <sup>31</sup>P NMR indicated the **6a** isomer to be the major component. Similar reaction at room temperature gave both isomers with **6b** being the major product. Both **6a** and **6b** were too unstable for further purifications.

**NiCl<sub>2</sub>[Cy<sub>2</sub>NPO]<sub>5</sub> (7).** A 2.6 g (3.8 mmol) amount of triphosphoxane and 0.60 g (2.7 mmol) of NiCl<sub>2</sub>·DME were stirred in 40 mL of hexane at room temperature. After 24 h, the dark-yellow suspension was filtered and the residue washed with

(24) Coucouvanis, D.; Salifoglou, A.; Kantzidis, M. G.; Dunham, W. R.; Simopoulos, A.; Kostikas, A. *Inorg. Chem.* **1988**, *27*, 4071. Gorzelli, M.; Nuber, B.; Ziegler, M. L. *J. Organomet. Chem.* **1992**, *436*, 207.

(25) Bennett, M. A.; Pratt, L.; Wilkinson, G. *J. Chem. Soc.* **1961**, 2037.

(26) King, R. B., Ed. *Organometallic Synthesis*; Academic Press: New York, 1965; p 124.

(27) King, R. B.; Fronzaglia, A. *Inorg. Chem.* **1966**, *5*, 1837.

(28) Abel, E. W.; Bennett, M. A.; Burton, R.; Wilkinson, G. *J. Chem. Soc.* **1958**, 4559.

(29) Ward, L. G. L. *Inorg. Synth.* **1972**, *13*, 154.

(30) McMullen, A. K.; Tilley, T. D.; Rheingold, A. L.; Geib, S. *J. Inorg. Chem.* **1990**, *27*, 2228. Brauer, G., Ed. *Handbook of Preparatory Inorganic Chemistry*; Academic Press: New York, 1965; Vol. 2, p 1547.

(31) Doyle, J. R.; Slade, P. E.; Jonassen, H. B. *Inorg. Synth.* **1960**, *6*, 218.

(32) McCrindle, R.; Alyea, E. C.; Ferguson, G.; Dias, S. A.; McAlees, A. J.; Parvez, M. *J. Chem. Soc., Dalton Trans.* **1980**, 137.

(33) Drew, D.; Doyle, J. R. *Inorg. Synth.* **1990**, *28*, 346.

hexane and then dissolved in  $\text{CH}_2\text{Cl}_2$ . This was filtered through Celite and the filtrate evaporated to give 1.65 g (48% based on Ni) of the yellow complex **7**. An analytical sample was prepared by recrystallization from toluene: IR,  $\nu_{\text{POP}}$  863  $\text{cm}^{-1}$ . Anal. Calcd for  $\text{C}_{60}\text{H}_{110}\text{Cl}_2\text{N}_5\text{NiO}_5\text{P}_5$ : N, 5.15; C, 59.24; H, 8.75. Found: N, 5.13; C, 59.26; H, 8.96.

**PdCl<sub>2</sub>[Cy<sub>2</sub>NPO]<sub>5</sub> (8A)**. Triphosphoxane (2.0 g, 2.9 mmol) and 0.60 g (1.5 mmol) of  $\text{PdCl}_2\cdot 2\text{PhCN}$  were refluxed in 40 mL of hexane for 12 h. The orange suspension turned yellow and was cooled and filtered. The yellow residue was washed with hexane and dried under reduced pressure to give 1.6 g (81% based on Pd) of **8A**: IR,  $\nu_{\text{POP}}$  868  $\text{cm}^{-1}$ . Anal. Calcd for  $\text{C}_{60}\text{H}_{110}\text{Cl}_2\text{N}_5\text{O}_5\text{P}_5\text{Pd}$ : N, 5.33; C, 54.85; H, 8.44. Found: N, 5.29; C, 54.49; H, 8.69.

**PdBr<sub>2</sub>[Cy<sub>2</sub>NPO]<sub>5</sub> (8B)**. A 0.90 g (1.3 mmol) amount of triphosphoxane and 0.30 g (0.60 mmol) of  $\text{PdBr}_2\cdot 2\text{PhCN}$  were refluxed in 40 mL of hexane for 12 h. Cooling of the yellow suspension, filtration, hexane washing, and drying of the residue gave the light-yellow solid **8B** (0.60 g, 71% based on Pd): IR,  $\nu_{\text{POP}}$  869  $\text{cm}^{-1}$ . Anal. Calcd for  $\text{C}_{60}\text{H}_{110}\text{Br}_2\text{N}_5\text{O}_5\text{P}_5\text{Pd}$ : N, 4.99; C, 51.38; H, 7.85. Found: N, 4.83; C, 51.45; H, 8.18.

**PtCl<sub>2</sub>[Cy<sub>2</sub>NPO]<sub>5</sub> (9)**. Triphosphoxane (0.44 g, 0.64 mmol) and 0.15 g (0.42 mmol) of  $\text{PtCl}_2(\text{NBD})$  were refluxed in 20 mL of hexane for 16 h. After cooling to room temperature and filtering, the white residue was washed with hexane and dried under reduced pressure to give about 0.47 g (80% based on Pt) of complex **9**. An analytical sample was obtained by recrystallization from toluene: IR,  $\nu_{\text{POP}}$  870  $\text{cm}^{-1}$ . Anal. Calcd for  $\text{C}_{60}\text{H}_{110}\text{Cl}_2\text{N}_5\text{O}_5\text{P}_5\text{Pt}$ : N, 4.69; C, 53.84; H, 7.96. Found: N, 4.67; C, 53.51; H, 8.42.

**Mo(CO)<sub>4</sub>[Pr<sub>2</sub>NPO]<sub>3</sub> (10A) and Mo(CO)<sub>4</sub>[Cy<sub>2</sub>NPO]<sub>3</sub> (10B)**. The synthesis and analyses of complex **10A** were described in ref 2. Complex **10B** was similarly prepared: The triphosphoxane  $[\text{Cy}_2\text{NPO}]_3$  (1.0 g, 1.5 mmol) and 0.40 g (1.3 mmol) of  $\text{Mo(CO)}_4(\text{NBD})$  were dissolved in 30 mL of hexane to give a yellow solution. After stirring for 2 h, a pale yellow suspension formed. The solid was filtered off, washed with cold hexane, and dried under reduced pressure to give 1.1 g (91% based on Mo) of white complex **10B**: IR,  $\nu_{\text{CO}}$  2000, 1918, 1889, 1885;  $\nu_{\text{POP}}$  826  $\text{cm}^{-1}$ . Anal. Calcd for  $\text{C}_{40}\text{H}_{66}\text{MoN}_3\text{O}_7\text{P}_3$ : N, 4.72; C, 53.99; H, 7.48. Found: N, 4.78; C, 53.66; H, 7.57.

**Cr(CO)<sub>4</sub>[Cy<sub>2</sub>NPO]<sub>4</sub> (11a)**. Triphosphoxane (1.6 g, 2.3 mmol) and  $\text{Cr(CO)}_4(\text{NBD})$  (0.20 g, 0.78 mmol) were refluxed in 50 mL of hexane for 40 h. Upon cooling to room temperature and standing overnight,  $\text{Cr(CO)}_6$  crystallized out and was filtered off. The solution was decolorized by stirring with alumina and filtering through Celite. The filtrate was then evaporated and the residue recrystallized from hot hexane to give 0.25 g (30% based on Cr) of complex **11a**: IR,  $\nu_{\text{CO}}$ , 2000, 1912, 1896, 1886  $\text{cm}^{-1}$ ;  $\nu_{\text{POP}}$  829  $\text{cm}^{-1}$ . Anal. Calcd for  $\text{C}_{52}\text{H}_{88}\text{CrN}_4\text{O}_8\text{P}_4$ : N, 5.22; C, 58.24; H, 8.21. Found: N, 5.12; C, 58.21; H, 8.35.

**Fe(CO)<sub>3</sub>[Cy<sub>2</sub>NPO]<sub>4</sub> (12)**. Triphosphoxane (0.60 g, 0.88 mmol) and  $\text{Fe}_2(\text{CO})_9$  (0.29 g, 0.80 mmol) were refluxed in 20 mL of hexane for 10 h. After cooling to room temperature and filtering through Celite, the filtrate was evaporated to dryness and the residue chromatographed on an alumina column using 2.5% ethyl acetate/hexane as the eluant. Complex **12** was isolated as a yellow solid and recrystallized from hot hexane to give 0.21 g (25% based on Fe) of **12**: IR,  $\nu_{\text{CO}}$  1995, 1926, 1899  $\text{cm}^{-1}$ ;  $\nu_{\text{POP}}$  832  $\text{cm}^{-1}$ . Anal. Calcd for  $\text{C}_{51}\text{H}_{88}\text{FeN}_4\text{O}_7\text{P}_4$ : N, 5.34; C, 58.43; H, 8.39. Found: N, 5.11; C, 58.77; H, 8.82.

**Fe(CO)<sub>3</sub>[Pr<sub>2</sub>NPO]<sub>4</sub> (13) and "Fe(CO)<sub>4</sub>[Pr<sub>2</sub>NPO]<sub>4</sub>" (14)**. Triphosphoxane (3.4 g, 7.7 mmol) and 2.0 g (5.5 mmol) of  $\text{Fe}_2(\text{CO})_9$  were refluxed in 60 mL of toluene for 18 h. After cooling and filtration through Celite, the filtrate was evaporated to dryness and the residue chromatographed on an alumina column using 2.5% ethyl acetate/hexane as the eluant. The yellow fraction was evaporated to dryness and recrystallized from hot hexane to give a mixture of large yellow cubic crystals of **13** and small light-yellow prisms of **14** suitable for X-ray

studies which were manually separated. Total yield of **13** and **14** was around 20% based on Fe. Anal. Calcd for **13**,  $\text{C}_{27}\text{H}_{56}\text{FeN}_4\text{O}_7\text{P}_4$ : N, 7.69; C, 44.54; H, 7.69. Found: N, 7.57; C, 44.32; H, 7.91. IR,  $\nu_{\text{CO}}$  1999, 1936, 1908  $\text{cm}^{-1}$ ;  $\nu_{\text{POP}}$  829  $\text{cm}^{-1}$ . Anal. Calcd for **14**,  $\text{C}_{28}\text{H}_{56}\text{FeN}_4\text{O}_8\text{P}_4$ : N, 7.41; C, 44.48; H, 7.41. Found: N, 7.38; C, 44.81; H, 7.57. IR,  $\nu_{\text{CO}}$  2047, 1987, 1947, 1933  $\text{cm}^{-1}$ ;  $\nu_{\text{POP}}$  875  $\text{cm}^{-1}$ .

**Cr(CO)<sub>4</sub>[Cy<sub>2</sub>NPO]<sub>4</sub> (11b), Cr<sub>2</sub>(CO)<sub>8</sub>[Cy<sub>2</sub>NPO]<sub>4</sub> (15), and Cr<sub>2</sub>(CO)<sub>7</sub>[Cy<sub>2</sub>NPO]<sub>5</sub> (16)**. The phosphine oxide  $(\text{Cy}_2\text{N})_2\text{P(O)H}$  (4.5 g, 11 mmol) and  $\text{Cr(CO)}_6$  (0.80 g, 3.6 mmol) were refluxed in 20 mL of toluene for 36 h. The dark-brown suspension was allowed to cool and then filtered through Celite. After evaporation of the filtrate, the residue was washed with about 20 mL of acetone and then extracted with 30 mL of hot hexane. The hexane extract was concentrated and chilled to precipitate about 0.61 g (32% based on Cr) of complex **11a**. The filtrate from this contained **11b** and **15** in about a 1:4 ratio according to its <sup>31</sup>P NMR spectrum. Further purification was not attempted. The acetone wash was evaporated to dryness and chromatographed on an alumina column using 0.5% ethyl acetate/hexane as the eluant. A first fraction contained a small amount of unstable  $\text{Cr(CO)}_5\text{OP(H)(NCy}_2)$  (IR,  $\nu_{\text{CO}}$  2047, 1975, 1927  $\text{cm}^{-1}$ ;  $\nu_{\text{P=O}}$  968  $\text{cm}^{-1}$ ) and the second gave 0.52 g (20% based on Cr) of **16** upon evaporation: IR,  $\nu_{\text{CO}}$  2005, 1961, 1930, 1905, 1892, 1875  $\text{cm}^{-1}$ ;  $\nu_{\text{POP}}$  900  $\text{cm}^{-1}$ . Anal. Calcd for  $\text{C}_{67}\text{H}_{110}\text{Cr}_2\text{N}_5\text{O}_{12}\text{P}_5$  (**16**): N, 4.88; C, 56.05; H, 7.72. Found: N, 4.43; C, 56.14; H, 8.22.

Complex **16** was also prepared by refluxing 4.5 g (11 mmol) of the phosphine oxide with  $\text{Cr(CO)}_6$  (0.80 g, 3.6 mmol) in 25 mL of xylene for 36 h. The dark brown suspension was cooled and filtered through Celite. The filtrate was evaporated to dryness and extracted with 30 mL of acetone. The acetone extract was dried under reduced pressure and chromatographed on an alumina column using 0.5% ethyl acetate/hexane eluant. A total of 1.7 g (65% based on Cr) of **16** was isolated.

**W<sub>2</sub>(CO)<sub>7</sub>[Cy<sub>2</sub>NPO]<sub>5</sub> (17) and W<sub>2</sub>(CO)<sub>6</sub>[Cy<sub>2</sub>NPO]<sub>4</sub> (18)**. An amount of the phosphine oxide (3.5 g, 8.6 mmol) and  $\text{W(CO)}_6$  (1.0 g, 2.8 mmol) was refluxed in 20 mL of toluene for 48 h. The dark-brown suspension was allowed to cool and filtered through Celite, and the filtrate was evaporated to dryness. The residue was chromatographed on an alumina column with hexane as the eluant. The first fraction to elute was the unstable yellow complex **17**, which was only characterized spectroscopically (Table 1). The second fraction yielded red crystalline complex **18** upon prolonged standing: IR,  $\nu_{\text{CO}}$  2000, 1973, 1930, 1908, 1904, 1876  $\text{cm}^{-1}$ ;  $\nu_{\text{POP}}$  885  $\text{cm}^{-1}$ . Anal. Calcd for  $\text{C}_{54}\text{H}_{88}\text{N}_4\text{O}_{10}\text{P}_4\text{W}_2$ : N, 3.56; C, 48.09; H, 6.93. Found: N, 3.59; C, 47.94; H, 7.20.

**Cr<sub>2</sub>(CO)<sub>8</sub>[DMP-PO]<sub>4</sub> (19a), Cr<sub>2</sub>(CO)<sub>8</sub>[DMP-PO]<sub>4</sub> (19b), and Cr(CO)<sub>7</sub>[DMP-PO]<sub>5</sub> (20)**. The phosphine oxide  $(\text{DMP})_2\text{P(O)H}$  (3.0 g, 11 mmol; synthesized from  $\text{DMP}_2\text{-PCL}$  in the same way as the dialkylaminophosphine oxides described in ref 2) and  $\text{Cr(CO)}_6$  (0.90 g, 4.1 mmol) were refluxed in 20 mL of toluene for 48 h. The dark-brown suspension was allowed to cool and filtered through Celite. The filtrate was evaporated to dryness and chromatographed on an alumina column using hexane eluant. The fraction collected was recrystallized from hexane to give complex **20** (0.28 g, 18% based on Cr): IR,  $\nu_{\text{CO}}$  2011, 1963, 1933, 1912, 1898, 1869  $\text{cm}^{-1}$ ;  $\nu_{\text{POP}}$  898  $\text{cm}^{-1}$ . The mother liquor was concentrated and a small amount of **19a** (0.10 g, 5%) crystallized out: IR,  $\nu_{\text{CO}}$  2006, 1942, 1892  $\text{cm}^{-1}$ ;  $\nu_{\text{POP}}$  819  $\text{cm}^{-1}$ . Prolonged standing gave 40 mg (2%) of large crystals of complex **19b**: IR,  $\nu_{\text{CO}}$  2004, 1927, 1908, 1897  $\text{cm}^{-1}$ ;  $\nu_{\text{POP}}$  881  $\text{cm}^{-1}$ . Anal. Calcd for  $\text{C}_{36}\text{H}_{56}\text{Cr}_2\text{N}_4\text{O}_{12}\text{P}_4$  (**19a**): N, 5.80; C, 44.80; H, 5.80. Found: N, 5.78; C, 45.11; H, 5.93. Calcd for  $\text{C}_{36}\text{H}_{56}\text{Cr}_2\text{N}_4\text{O}_{12}\text{P}_4$  (**19b**): N, 5.80; C, 44.80; H, 5.80. Found: N, 5.77; C, 45.07; H, 6.04. Calcd for  $\text{C}_{42}\text{Cr}_2\text{H}_{70}\text{N}_5\text{O}_{12}\text{P}_5$ : N, 5.78; C, 49.61; 7.33. Found: N, 5.96; C, 49.35; H, 6.95.

**Cr<sub>2</sub>(CO)<sub>6</sub>[DMP-PO]<sub>6</sub> (21)**. Phosphine oxide (0.10 g, 0.37 mmol) and  $\text{Cr}_2(\text{CO})_7[\text{DMP-PO}]_5$  (complex **20**; 0.10 g, 0.090

Table 9. Crystallographic Data for Complexes 14, 19a, 19b, 21, and 25

	14	19a	19b	25	21
(a) Crystal Parameters					
formula	C <sub>28</sub> H <sub>56</sub> FeN <sub>4</sub> O <sub>8</sub> P <sub>4</sub>	C <sub>36</sub> H <sub>56</sub> Cr <sub>2</sub> N <sub>4</sub> O <sub>12</sub> P <sub>4</sub>	C <sub>36</sub> H <sub>56</sub> Cr <sub>2</sub> N <sub>4</sub> O <sub>12</sub> P <sub>4</sub>	C <sub>34</sub> H <sub>62</sub> FeMoN <sub>4</sub> O <sub>11</sub> P <sub>4</sub>	C <sub>56</sub> H <sub>94</sub> Cr <sub>2</sub> N <sub>6</sub> O <sub>12</sub> P <sub>6</sub>
formula weight	756.5	964.7	964.7	978.5	1333.2
crystal system	monoclinic	monoclinic	triclinic	monoclinic	triclinic
space group	<i>C2/c</i>	<i>I2/c</i>	<i>P1̄</i>	<i>P2<sub>1</sub>/c</i>	<i>P1̄</i>
<i>a</i> , Å	42.583(14)	27.593(8)	9.905(3)	20.200(13)	10.650(2)
<i>b</i> , Å	13.298(4)	18.105(7)	11.668(4)	12.003(4)	12.407(3)
<i>c</i> , Å	14.828(4)	18.648(5)	12.189(3)	21.881(12)	13.064(3)
$\alpha$ , deg			96.62(2)		106.64(2)
$\beta$ , deg	109.48(3)	91.45(2)	110.81(2)	117.45(2)	93.60(2)
$\gamma$ , deg			112.59(2)		95.92(2)
<i>V</i> , Å <sup>3</sup>	7916.3(4)	9313	1162.9(5)	4708(4)	1637.3(6)
<i>Z</i>	8	8	1	4	1
cryst dims, mm	0.25 × 0.28 × 0.44	0.40 × 0.40 × 0.45	0.40 × 0.40 × 0.45	0.25 × 0.30 × 0.30	0.18 × 0.30 × 0.60
cryst color	yellow	colorless	yellow	colorless	colorless
<i>D</i> <sub>calc</sub> , g cm <sup>-3</sup>	1.270	1.376	1.378	1.381	1.352
$\mu$ (Mo K $\alpha$ ), cm <sup>-1</sup>	5.89	6.47	6.47	7.64	5.39
temp, K	244	296	296	233	237
(b) Data Collection					
diffractometer			Siemens P4		
monochromator			graphite		
radiation			Mo K $\alpha$ ( $\lambda = 0.71073$ Å)		
$2\theta$ scan range, deg	4.0–52.0	4.0–52.0	4.0–52.0	4.0–54.0	4.0–50.0
data collected ( <i>h, k, l</i> )	±49, +16, +18	±34, +22, +22	±12, ±14, +15	±22, +15, +27	±12, ±14, +15
no. of coll'd rflns	8467	9465	4799	11220	6055
no. of ind rflns	7747	9164	4571	11043	5778
no. of ind obsd rflns	4391	5611	3489	5730	4515
$F_o \geq n\sigma(F_o)$ ( $n = 4$ )					
std rflns	3 std/197 rflns	3 std/197 rflns	3 std/197 rflns	3 std/197 rflns	3 std/197 rflns
var in std, %	2	<1	2	1	2
(c) Refinement					
<i>R</i> ( <i>F</i> ), %	6.08	5.89	4.81	5.49	4.66
<i>R</i> ( <i>wF</i> ), %	6.97	6.95	6.99	5.72	5.19
$\Delta/\sigma$ (max)	0.031	0.598	0.108	0.549	0.054
$\Delta(\rho)$ , eÅ <sup>-3</sup>	0.67	1.10	1.02	0.65	0.94
<i>N</i> <sub>o</sub> / <i>N</i> <sub>v</sub>	10.8	10.7	13.3	11.3	12.9
GOF	1.28	1.35	1.20	1.10	1.44

mmol) were refluxed in 20 mL of xylene for 6 h. After cooling to room temperature and filtration, the solid residue was recrystallized from toluene to give 0.10 g (90% based on **20**) of complex **21**: IR,  $\nu_{CO}$  1949, 1893, 1876 cm<sup>-1</sup>;  $\nu_{POP}$  912 cm<sup>-1</sup>. Slow cooling of a hot xylene solution of **21** gave X-ray quality crystals. Anal. Calcd for C<sub>48</sub>H<sub>84</sub>Cr<sub>2</sub>N<sub>4</sub>O<sub>12</sub>P<sub>4</sub>·2toluene: N, 5.96; C, 52.79; H, 7.09. Found: N, 5.82; C, 52.21; H, 7.14.

**Mo<sub>2</sub>(CO)<sub>8</sub>[DMP-PO]<sub>4</sub> (22).** The phosphine oxide (DMP)<sub>2</sub>P(O)H (1.0 g, 3.6 mmol) and 0.50 g Mo(CO)<sub>6</sub> (1.8 mmol) were refluxed in 20 mL of toluene for 48 h. The dark-brown suspension was cooled, filtered through Celite, and the filtrate was evaporated to dryness. Chromatography of the residue on an alumina column using hexane yielded a white solid. It was recrystallized from hexane to give 0.31 g (32% based on Mo) of **22**: IR,  $\nu_{CO}$  2012, 1928, 1914, 1898 cm<sup>-1</sup>;  $\nu_{POP}$  885 cm<sup>-1</sup>. Anal. Calcd for C<sub>36</sub>H<sub>56</sub>Mo<sub>2</sub>N<sub>4</sub>O<sub>12</sub>P<sub>4</sub>: N, 5.32; C, 41.09; H, 5.32. Found: N, 5.28; C, 41.19; H, 5.50.

**Mo(CO)<sub>4</sub>[Cy<sub>2</sub>NPO]<sub>4</sub>NiBr<sub>2</sub> (23).** The complex NiBr<sub>2</sub>[Cy<sub>2</sub>NPO]<sub>4</sub> (0.45 g, 0.40 mmol of **8A**) and Mo(CO)<sub>4</sub>(NBD) (0.12 g, 0.40 mmol) were stirred in 25 mL of toluene at 90 °C for 3 h. The clear red solution turned pale brown as the reaction progressed. After cooling and filtration through Celite, the filtrate was evaporated and the residue chromatographed on an alumina column using 2.5% ethyl acetate/hexane as the eluant. The red-brown solid isolated was 0.25 g (47% based on Mo) of complex **23**: IR,  $\nu_{CO}$  2022, 1945, 1928, 1909 cm<sup>-1</sup>;  $\nu_{POP}$  904 cm<sup>-1</sup>. Anal. Calcd for C<sub>52</sub>H<sub>88</sub>Br<sub>2</sub>MoN<sub>4</sub>NiO<sub>8</sub>P<sub>4</sub>: N, 4.19; C, 46.79; H, 6.59. Found: N, 4.10; C, 46.76; H, 6.87.

**Mo(CO)<sub>3</sub>[Cy<sub>2</sub>NPO]<sub>5</sub>PdCl<sub>2</sub> (24).** The complex PdCl<sub>2</sub>[Cy<sub>2</sub>NPO]<sub>5</sub> (0.26 g, 0.20 mmol of **8A**) and Mo(CO)<sub>4</sub>(NBD) (60 mg, 0.20 mmol) were stirred in 30 mL of toluene at 90 °C for 5 h. After cooling to room temperature and filtration through Celite, the filtrate was evaporated to dryness. The residue was then chromatographed on an alumina column using 5%

ethyl acetate/hexane eluant. The pale-yellow solid complex **24** was isolated (0.12 g, 40% based on Mo): IR,  $\nu_{CO}$  1979, 1912, 1902, 1890 cm<sup>-1</sup>;  $\nu_{POP}$  919 cm<sup>-1</sup>. Anal. Calcd for C<sub>63</sub>H<sub>110</sub>Cl<sub>2</sub>MoN<sub>5</sub>O<sub>8</sub>P<sub>5</sub>Pd: N, 4.69; C, 50.69; H, 7.37. Found: N, 4.36; C, 50.41; H, 7.78.

**Mo(CO)<sub>4</sub>[Pr<sub>2</sub>NPO]<sub>4</sub>Fe(CO)<sub>3</sub> (25).** The complex Fe(CO)<sub>3</sub>-[Pr<sub>2</sub>NPO]<sub>4</sub> (0.20 g, 0.27 mmol of **13**) and Mo(CO)<sub>4</sub>(NBD) (0.10 g, 0.33 mmol) were refluxed in 20 mL of hexane for 5 h. After cooling, the solution was evaporated to dryness and chromatographed on an alumina column using 0.5% ethyl acetate/hexane as the eluant. The isolated product was recrystallized from benzene/hexane to give 0.19 g (75% based on Fe) of **25** as pale yellow crystals suitable for X-ray analysis: IR,  $\nu_{CO}$  2021, 1999, 1962, 1944, 1922, 1912, 1899, 1877, 1869 cm<sup>-1</sup>;  $\nu_{POP}$  873 cm<sup>-1</sup>. Anal. Calcd for C<sub>31</sub>H<sub>56</sub>FeMoN<sub>4</sub>O<sub>11</sub>P<sub>4</sub>: N, 5.98; C, 39.78; H, 5.98. Found: N, 6.03; C, 39.83; H, 5.98.

**Ni(CO)<sub>2</sub>[Cy<sub>2</sub>NPO]<sub>4</sub>Ni(CO)<sub>2</sub> (26).** NiBr<sub>2</sub>[Cy<sub>2</sub>NPO]<sub>4</sub> (1.50 g, 1.3 mmol) and Fe<sub>2</sub>(CO)<sub>9</sub> (0.48 g, 1.3 mmol) were stirred in 40 mL of toluene at 90 °C. After 2 h, the suspension was cooled to room temperature and filtered through Celite. The filtrate was evaporated to dryness and the residue chromatographed on an alumina column using 2.5% ethyl acetate/hexane eluant. A yield of 0.27 g (18% based on Ni) of white complex **26** was isolated: IR,  $\nu_{CO}$  2000, 1947 cm<sup>-1</sup>;  $\nu_{POP}$  870 cm<sup>-1</sup>. Anal. Calcd for C<sub>52</sub>H<sub>88</sub>N<sub>4</sub>Ni<sub>2</sub>O<sub>8</sub>P<sub>4</sub>: N, 4.92; C, 54.89; H, 7.73. Found: N, 4.71; C, 54.87; H, 8.11.

**Crystallographic Studies.** Crystal, data collection, and refinement parameters are listed in Table 9. Single crystals of complexes **14**, **19a**, and **19b** were grown from saturated hexane solutions. Crystals of **21** and **25** were from xylene and benzene, respectively. Suitable crystals were selected and mounted on glass fibers with epoxy cement. The unit cell parameters were obtained by least-squares refinement of the

angular settings of 25 reflections ( $20^\circ \leq 2\theta \leq 25^\circ$ ). The XABS program was used to correct the data for absorption for **25**.<sup>34</sup>

The systematic absences in the diffraction data for **14** are consistent for space groups  $C2/c$  and  $Cc$ ; for **19a**,  $I2/a$  and  $Ia$ ; for **19b** and **21**,  $P1$  and  $P1$ ; and uniquely for **25**,  $P2_1/c$ . The  $E$ -statistics suggested the centrosymmetric alternatives for **14**, **19a**, **19b**, and **21** and were verified by subsequent refinements.

The centers of the molecules of **19b** and **25** are located on inversion centers. In **21** and **25**, several peaks on the Fourier difference maps, not connected with the compound molecules, were observed and modeled as *p*-xylene and benzene, respectively. These solvent molecules were isotropically refined.

All structures were solved by direct methods, completed by subsequent difference Fourier syntheses, and refined by full-matrix least-squares procedures. All non-hydrogen, nonsol-

vent atoms were refined with anisotropic displacement coefficients. Hydrogen atoms were treated as idealized contributions.

All software and sources of the scattering factors are contained in either in SHELXTL (5.1) or the SHELXTL PLUS (4.2) program libraries (G. Sheldrick, Siemens XRD, Madison, WI).

**Acknowledgment.** We acknowledge financial support from the Petroleum Research Fund, administered by the American Chemical Society.

**Supplementary Material Available:** Listings of atomic coordinates, anisotropic thermal factors, and complete bond distances and angles (35 pages). Ordering information is given on any current masthead page.

---

(34) Hope, H.; Moezzi, B., University of California, Davis, CA.

OM940442H